IMA Journal of Applied Mathematics (2018) Page 1 of 36
doi:10.1093/imamat/iarxxx

Trapped modes of the Helmholtz equation in infinite waveguides with wall indentations and circular obstacles

CRISTINA SARGENT*
Imperial College London
*cristina.sargent04@imperial.ac.uk

AND

A.J. MESTEL**
Imperial College, London
**j.mestel@imperial.ac.uk

[Received on XX XX XXXX; revised on XX XX XXXX; accepted on XX XX XXXX]

Trapped modes of the Helmholtz equation are investigated in infinite, two-dimensional acoustic waveguides with Neumann or Dirichlet walls. A robust boundary element scheme is used to study modes both inside and outside the continuous spectrum of propagating modes. An effective method for distinguishing between genuine trapped modes and spurious solutions induced by the domain truncation is presented. The method is also suitable for the detection and study of "nearly trapped modes" (NTM). These are of great practical importance as they display many features of trapped modes but do not require perfect geometry.
An infinite, two-dimensional channel is considered with one or two discs on its centreline. The walls may have rectangular, triangular or smooth cavities. The combination of a circular obstacle and a rectangular cavity, in both Neumann and Dirichlet guides is studied, illustrating the possible use of a movable disc to detect wall irregularities.
The numerical method is validated against known results and many new modes are identified, both inside and outside the continuous spectrum. Results obtained suggest that at least one symmetry line is an important condition for the formation of trapped mode type resonances. The addition of a symmetry-preserving geometric parameter to a problem which has a discrete embedded trapped mode solution for a specific geometry, tends to lead to a continuous set of trapped modes.

Keywords: trapped modes, defect detection, Helmholtz equation, bound states, acoustic resonances

2000 Math Subject Classification: 34K30, 35K57, 35Q80, 92D25

1. Introduction

Within the framework of classical wave theory, trapped modes are time-harmonic oscillations at some well-defined frequency, which are localised near a boundary or trapping structure in unbounded domains. The decay with distance from the trapping feature is usually exponential although algebraic decay can also occur. Mathematically, a trapped mode corresponds to an eigenfunction with no radiation to the far field. Over the past 60 years the study of trapped modes has intensified and diversified. Depending on the context, trapped modes are known as acoustic resonances, Rayleigh-Bloch waves, edge waves, array guided surface waves, sloshing modes, motion trapped modes and quantum mechanical bound states.

Trapped modes are considered here in an acoustic context, but direct comparison can be made with associated problems in water-waves and in quantum waveguides Callan et al. (1991), Evans et al. (1993),

Evans & Porter (1999), Exner & Seba (1989), Postnova & Craster (2008) and in cyclotrons Caspers & Scholz (1996).

In this paper we shall consider waves in a two-dimensional channel $|y| < d$ which acts as a waveguide. Time-harmonic oscillations with angular frequency $\omega = kc$ are considered, where c is the wavespeed. The pressure fluctuation in the guide, ϕ, satisfies the Helmholtz equation $\nabla^2\phi + k^2\phi = 0$, subject to appropriate homogeneous boundary conditions. We shall consider both Dirichlet and Neumann wall conditions. A trapped mode (or acoustic resonance) is a solution for ϕ in an infinite domain with finite energy. The positive value of the wavenumber k for which a solution exists is referred to as the trapped mode frequency.

Trapped modes can be classified as embedded or non-embedded, depending on whether their frequency is respectively above or below the first cut-off for travelling modes. This distinction is important as it determines the stability of the mode. The non-embedded modes are stable in the sense that if a geometric parameter is varied continuously, the mode persists up to some limit, with only a slight variation of its frequency. In contrast, embedded modes may exist only for a specific combination of the geometric parameters and may be formally destroyed by an infinitesimal perturbation of the configuration, giving rise to NTMs. This means that for many configurations, embedded modes may not exist at all, or there may be only a few discrete geometric parameter values which support such a mode. From a computational perspective the distinction is important because embedded trapped modes require higher detection accuracy than non-embedded modes as an eigenvalue in the continuous spectrum disappears under small perturbations. Nevertheless, the NTM frequencies are of practical importance.

There is a vast amount of literature on analytical, numerical and physical aspects of trapped mode problems, to which it is hard to do justice. We mention here a few results and relevant notions, but our coverage is far from exhaustive.

Historically, trapped modes were first discovered in failed attempts to prove uniqueness. For a specified geometry, uniqueness of the solution to a forced problem at a particular frequency is equivalent to the non-existence of a trapped mode at that frequency. For the difference between two such solutions is a non-trivial solution of the homogeneous problem, i.e. a trapped mode.

John (1950) established uniqueness for a particular class of single, surface-piercing bodies which have the property that any vertical line emanating from the free surface does not intersect the body. Ursell (1950) proved uniqueness for a circular cylinder submerged in fluid of infinite depth. Since then many other partial results have been obtained (see, for example, Simon & Ursell (1984)) but a general proof of uniqueness for all bodies at all frequencies was not found. The reason for the absence of such a proof soon became clear. For example, McIver (1996), constructed an explicit example of two surface-piercing bodies for which the potential is non-unique at a specific frequency. Detailed reviews of the literature are provided by Linton & McIver (2007) and Kuznetsov et al. (2002).

An alternative conception of the problem began with Ursell (1951), who established the correspondence between the finite energy of a trapped mode and the type of eigenvalue which gives rise to it. If a fluid is bounded by fixed surfaces and by a free surface of infinite extent, the modes of vibration with infinite energy form a continuous spectrum. A trapped mode has finite total energy and corresponds to a discrete eigenvalue embedded within the continuous spectrum. In a subsequent study, Jones (1953) established that semi-infinite domains which are cylindrical at infinity have a continuous spectrum with a discrete embedded spectrum. Jones' work established the Helmholtz equation, with suitable boundary conditions, as a rich mathematical area for the study of trapped modes which we continue in this paper.

Waveguides with one or more obstacles of various shapes, placed either symmetrically with respect to the centreline or off-centre, have been much studied in various contexts as the problem has important applications. The configuration is mathematically equivalent to that of an infinite periodic array of such

obstacles. Finite arrays of structures may exhibit "nearly" trapped modes. These consist in practice of large amplitude responses to forcing near the trapped mode frequencies of the corresponding infinite array. A typical example would be the support columns of a long bridge, which can be represented as two discs in a waveguide, e.g. Chen et al. (2012).

The existence of trapped modes in two-dimensional infinite acoustic waveguides with an obstruction of general shape, symmetric about the centreline of the guide, was established by Evans et al. (1994). Associated calculations for a sound-hard disc (i.e. with Neumann condition on its boundary) at the centre of Neumann and Dirichlet guides (i.e. with Neumann or Dirichlet boundary condition on the guide walls respectively) were reported in Callan et al. (1991), Evans & Porter (1997b) and Maniar & Newman (1997).

Callan et al. (1991) constructed the solution for the case of one disc of radius a placed at the centre of an infinite Neumann guide of width $2d$, using a linear combination of suitably modified multipole potentials. It was shown that for each a/d there is a particular wavenumber below the first cut-off $\pi/2d$ which satisfies the Neumann trapped mode problem. Additional modes, for a linear array of discs with $0.81 \lesssim a/d$, were reported by Evans & Porter (1999). These findings are consistent with the analysis of Cobelli et al. (2011), who reproduced this case experimentally and reported two resonance curves for discs such that $0.8 \leqslant a/d \leqslant 1$. Extending the work of Callan *et al.*, Evans & Porter (1997b) established that one embedded mode, in the range $\pi/2 \leqslant kd \leqslant 3\pi/2$ exists for only one value $a/d \approx 0.352$ and a corresponding $kd \approx 4.677 \approx 1.489\pi$.

For an infinite Dirichlet waveguide, without any symmetry considerations, the first cut-off is $kd = \pi/2$. For soft waveguides it was proved by McIver & Linton (1995) that trapped modes do not exist below the first cut-off frequency for a large class of of both sound-soft and sound-hard bodies. In addition, they showed that antisymmetric trapped modes do not exist below the first cut-off in many two-dimensional Neumann guides containing sound-soft bodies if they satisfy the condition $n_y \leqslant 0$ if $y \geqslant 0$, and $n_y \geqslant 0$ if $y \leqslant 0$ (where (n_x, n_y) is the normal to the obstacle out of the fluid region). A large class of obstacles satisfy this geometrical condition, including discs and rectangular blocks symmetrically placed with respect to the guide walls. But if the trapped modes sought are antisymmetric about the centreline then the continuous spectrum of the problem is the interval $k \in [\pi/d, \infty)$ and non-embedded modes can be found below the first cut-off π/d.

Maniar & Newman (1997) found that one antisymmetric trapped mode, with frequencies $\pi/2 < kd < \pi$ exists for each disc in a Dirichlet waveguide, such that $0 < a/d \lesssim 0.6788$. For $\pi < kd < 2\pi$, a trapped mode exists for the isolated value of $a/d \approx 0.267$, at a frequency $kd \approx 6.258 \approx 1.992\pi$ - see Evans & Porter (1997b) and Linton & McIver (2007). For multiple cylinders on the centreline of either a Dirichlet or Neumann guide, non-embedded trapped mode results are given by Evans & Porter (1997a).

Following these initial results establishing their existence, trapped modes were discovered in many contexts, from large physical structures supported by arrays of standing columns to quantum waveguides and nanowire inclusions in metamaterials Podolskiy et al. (2003). Given their wide applicability, from non-destructive testing to enhancement of evanescent modes in the near-field of a "perfect lens" Pendry (2000, 2004), systematic and efficient numerical methods of detection of trapped modes are required.

Various numerical schemes have been used to investigate trapped modes. A difficulty every method faces relates to the need to truncate an infinite domain, applying an appropriate boundary condition on some finite boundary. As the trapped solutions decay at large distances it would not seem critical how this is done. Yet every simple scheme gives rise to spurious resonances, which must be eliminated carefully. Any single spurious mode for a particular geometry can be identified and culled by varying the numerical truncation and discretisation. But automatic and efficient investigation of a wide parameter space is a challenge.

We formulate the problem in §2 and present in §3 a numerical approach based on the boundary element method (BEM) which we use to find trapped modes in two-dimensional waveguides. There are two main ideas behind this scheme. Firstly, assuming exponential decay along the guide, the dominant exponential decay condition is imposed at some length $x = L$. Secondly, we obtain a measure of the radiation down the pipe for any candidate solution and insist that this be small, noting that trapped and nearly trapped modes give a sharp minimum of this measure. The combination of these two conditions automatically weeds out the spurious modes while permitting a moderately small value of L. This novel combination turns out to be well-suited to investigate the higher frequency embedded modes where the presence of propagating modes renders other methods less effective. It also identifies NTMs well. Naturally, distinguishing between trapped and nearly trapped modes requires greater accuracy, but the general vicinity of such modes is located efficiently.

Other procedures have been employed for the numerical detection of trapped modes, for example Hardy space element techniques Hohage & Nannen (2015) and finite elements combined with perfectly matched layers (PML), e.g. Duan et al. (2007); Hein & Koch (2008). PMLs are advantageous in some problems, but we consider our BEM approach more appropriate for trapped mode detection. The BEM is computationally efficient as it calculates the solution in terms of values attained on the domain boundary, therefore reducing computations by one dimension. As against this, the matrix in the BEM formulation is 'full', whereas for the PML approach it is sparse, albeit in one more dimension. The PML methods work well for scattering problems, but the BEM procedure appears more robust for trapped mode detection as it automatically avoids the difficulties reported by Duan et al. (2007) whereby the discrete numerical eigenvalues, which are strongly dependent on the PML parameters, can be mistaken for resonant eigenvalues thus rendering it very difficult to distinguish between the two. Our scheme is designed to be flexible and computationally efficient to allow the study of trapped modes in geometries without symmetry, e.g. with cavities and obstacles which are not aligned with each other.

In §4, we use the method for one or more sound-hard circular discs in both Neumann and Dirichlet guides. We have reproduced those results obtained by other authors using different methods, for a wide range of confugurations and extend those results in both the embedded and nonembedded frequency regimes.

In §5, guides with wall cavities are considered. The trapped modes for this problem can be regarded either as resonances in soft acoustic guides or as bound states in quantum waveguides Exner & Seba (1989), Carini et al. (1992). The latter are narrow, two dimensional quantum guides, composed of tiny strips of a very pure semiconductor material, that allow electrons to propagate but require the wave function to vanish on the surface.

The trapped modes for a Dirichlet guide with a rectangular or Gaussian cavity are found for frequencies up to the second cut-off. We do not discuss symmetrical indentations in each guide wall, e.g. Fernyhough (1998). A Neumann waveguide with rectangular or triangular cavity is also investigated. Neumann guides with cavities have received much attention, e.g.Duan et al. (2007). We include here one such example for illustration and as a logical precursor to the next section.

In §6 a sound-hard disc, aligned with the rectangular cavity, is added to both Dirichlet and Neumann guides. This could be regarded as a mobile detection device, sent down the channel to detect wall imperfections. The addition of new geometric parameters to a problem which has one embedded trapped mode for a specific discrete geometry, leads to the appearance of a continuous set of solutions. The behaviour of the trapped frequencies as the disc is moved provides information about the cavity and its location.

Geometries without any (x,y) symmetry, consisting of Dirichlet and Neumann guides with a rectangular cavity and a sound-hard disc removed from the guide centre (not aligned with the cavity anymore)

are also considered. We have not identified any genuinely trapped modes for geometries without a symmetry line, although Nazarov (2013) has shown that these exist.

§7 is concerned with nearly trapped modes (NTMs) as they were consistently found throughout our computations. Indeed, for an isolated trapped mode, any approximation to it would be a NTM. In some cases, NTMs may be correspond to a complex eigenvalue of the infinite problem, but we do not pursue that approach here. Unlike pure trapped modes, which have zero radiation, NTMs are near-resonances with small radiation. The BEM developed is ideally suited for their detection. Although NTMs are not a solution to the infinite problem in that they do not satisfy the decay condition in the far field, they are important because of their practical implications. The high amount of energy present in the near field, in comparison with the amount that radiates, is important in predicting the forces on the trapping features. We conclude in §8.

2. Mathematical formulation

The domain is an infinite waveguide (W) consisting of a pair of planar walls ($\Gamma_\pm$) at $y=\pm d$ and a trapping feature (D) consisting of one or more sound-hard discs on the guide's centreline. In some cases the trapping feature consist of a cavity in one of the planar walls. All geometric parameters are henceforth scaled by d for ease of notation, so that $d=1$ and all subsequent spatial variables are non-dimensional. All symmetry descriptions, unless otherwise specified, refer to the x direction.

The trapped mode problem, either Dirichlet or Neumann, for the reduced velocity potential $\phi(x,y)$, is formulated as follows:

$$(\nabla^2+k^2)\phi=0 \quad \text{for} \quad (x,y)\in W\backslash D \tag{2.1}$$

$$\phi\to 0 \quad \text{for} \quad |x|\to\infty,\ |y|\leqslant 1 \tag{2.2}$$

$$\frac{\partial\phi}{\partial n}=0 \quad \text{for} \quad (x,y)\in \partial D \tag{2.3}$$

$$\text{Dirichlet problem:} \quad \phi=0 \quad \text{for} \quad (x,y)\in\Gamma_\pm \quad \text{or} \tag{2.4}$$

$$\text{Neumann problem:} \quad \frac{\partial\phi}{\partial y}=0 \quad \text{for} \quad (x,y)\in\Gamma_\pm \tag{2.5}$$

where $\partial/\partial n$ is the outward normal derivative. In this formulation k^2 is an eigenvalue of either the Dirichlet or Neumann problem if it corresponds to a non-trivial solution ϕ which satisfies either (2.1) - (2.4) or (2.1) - (2.3) and (2.5) respectively.

The governing equations are translated into a flexible procedure which allows analysis of any two dimensional domain and can be applied to both internal and external problems. Using standard techniques of potential theory (2.1) is re-written as an integral equation. For any point $\mathbf{x}'$ on the boundary $\Gamma_\pm\cup\partial D$, the space dependent potential $\phi(\mathbf{x}')$, can be written in terms of boundary integrals

$$c(\mathbf{x}')\,\phi(\mathbf{x}')=\int_{\Gamma_\pm\cup\partial D}\left[\phi(\mathbf{x})\frac{\partial G(\mathbf{x},\mathbf{x}')}{\partial n}-G(\mathbf{x},\mathbf{x}')\frac{\partial\phi(\mathbf{x})}{\partial n}\right]\mathrm{ds}(\mathbf{x}). \tag{2.6}$$

The free coefficient $c(\mathbf{x}')$ is given by

$$c(\mathbf{x}')=\frac{\alpha}{2\pi},\quad 0\leqslant c(\mathbf{x}')\leqslant 1, \tag{2.7}$$

where α is the the angle subtended at the point of interest $\mathbf{x}'$. For this two-dimensional problem, we use for $G(\mathbf{x},\mathbf{x}')$ the fundamental solution $G=\frac{1}{4i}H_0^1(k|\mathbf{x}-\mathbf{x}'|)$, where H_0^1 is the Hankel function of the first

kind and zeroth order. If all calculations were in a regular waveguide, one could instead use the periodic Green's function Linton (1998) and McIver et al. (2001) but we wish our method also to apply to more general geometry.

The infinite waveguide is truncated to a finite section such that $-1 \leqslant y \leqslant 1, -L \leqslant x \leqslant L$. The distance L must be sufficiently large to reach into the far field where the solution decay is dominant. The truncated boundary is divided into N small line elements S_m, $(m = 0, 1, \ldots N)$, of length l. The choice of l depends on the precision necessary for the detection of a mode, the embedded modes requiring finer boundary discretisation than the non-embedded. A simple comparison between known analytic results and numeric solutions obtained with our program, confirms that the error in the trapped mode frequency values is proportional to N^{-2}, as expected. The majority of results presented here were obtained using boundary elements of length $0.01 \leqslant l \leqslant 0.1$.

Following the discretisation step, the right hand side of (2.6) is reduced to a summation of N integrals over each boundary element

$$c(\mathbf{x}')\phi(\mathbf{x}') = \sum_{m=1}^{N} \left\{ \int_{S_m} \left[\phi(\mathbf{x}) \frac{\partial G(\mathbf{x}, \mathbf{x}')}{\partial n} - G(\mathbf{x}, \mathbf{x}') \frac{\partial \phi(\mathbf{x})}{\partial n} \right] ds(\mathbf{x}) \right\}, \quad \mathbf{x}' \in S_m. \tag{2.8}$$

On each segment either ϕ or $\partial\phi/\partial n$ is known. The remaining unknown is expressed as a linear function of its values at the end points of the segment. The discretised equation (2.8) is used to express ϕ at each of the N points along the boundary. With the application of boundary conditions, a system of N equations in N unknowns is obtained. The system is written in matrix form as

$$M\mathbf{X} = 0. \tag{2.9}$$

The complex entries in $M(k)$ are obtained by integrating the terms in (2.8) along each boundary element S_m. The vector $\mathbf{X}$ stores the unknown values of either the potential or its normal derivative on each of element S_m. The existence of non-trivial solutions requires that $\det[M(k)] = 0$. Without loss of generality, $\mathbf{X}$ can be chosen to be real within the bounds of numerical error. Hence, solutions correspond to those frequencies for which both the real and the imaginary parts of the matrix are simultaneously singular i.e.

$$\det[M_R(k)] = 0 \text{ and } \quad \det[M_I(k)] = 0. \tag{2.10}$$

respectively. These two conditions are used by the program to verify the accuracy of the calculations and provide a more robust investigation tool. For this problem it would be possible to have chosen a real fundamental solution for G, but the actual choice provides a valuable diagnostic and accuracy check. It also facilitates extension towards calculating complex resonances in other problems. Further details concerning computation accuracy including the treatment of singularities can be found in Sargent (2012). Discussion of the general principles of the boundary element method can be found in Brebbia et al. (1984).

3. Identification of trapped modes

The trapped mode condition (2.2) defined at infinity cannot be tested directly on a finite domain. Instead, on the edges where the domain is truncated, the following decay conditions are imposed

$$\frac{\partial \phi}{\partial x} \sim \mu_1 \phi,\ x = -L \quad \text{and} \quad \frac{\partial \phi}{\partial x} \sim -\mu_1 \phi,\ x = L, \quad -1 \leqslant y \leqslant 1. \tag{3.1}$$

The decay coefficient μ_1 depends on the problem and the range of frequencies investigated. This choice of boundary condition is based on the assumption that in the positive far field for a given trapped mode frequency, the solution can be written as an infinite superposition of modes, which satisfy the boundary conditions on $\pm\Gamma$. Taking the Neumann case with $0 < k < \pi/2$, for example

$$\phi = \sum_{n=1}^{\infty} a_n e^{-\mu_n x} \sin\left[\frac{(2n-1)\pi}{2} y\right], \quad \mu_n = \left[\left(\frac{2n-1}{2}\pi\right)^2 - k^2\right]^{\frac{1}{2}}. \tag{3.2}$$

A similar expansion is used in Wang (2014). In the positive far field the solution is expected to behave asymptotically as

$$\phi \approx a_1 e^{-\mu_1 x} \sin\frac{\pi y}{2}. \tag{3.3}$$

With regard to (3.2), we see that condition (3.1) introduces an error proportional to $\exp[-(\mu_2 - \mu_1)L]$. In contrast, a homogeneous Dirichlet condition, say, would make an error of $O(\exp(-\mu_1 L))$ which can be much greater, given the typical proximity of k to $(n-1/2)\pi$. This effectively permits equivalent accuracy to be obtained for much smaller values of L. The substitute condition (3.1) successfully identifies the decaying solutions but also allows standing waves with wavenumbers which satisfy the boundary condition at $x = \pm L$ exactly, yielding a spurious set of eigenvalues which do not satisfy (2.2). For example solutions of the form $\cos(\sqrt{\pi^2/4 - k^2}x)\sin(\pi y/2)$ could occur where k satisfies both (3.1) and (3.3) at $x = L$.

A simple but computationally inefficient way to identify these spurious modes would be to vary the truncation length L, over which the computation is carried out. An eigenvalue corresponding to a genuine trapped mode is not dependent on the truncation of the guide whereas the k values of spurious modes do vary greatly with L. Plotting the determinants of $M_R(k)$ and $M_I(k)$ for increasing number of discretisation points N, can also differentiate between genuine and some fictitious solutions, as the wavenumbers obtained for a real trapped mode should converge to the real solution. However, both these strategies, although reliable, are time consuming when applied to wide ranges of frequencies and geometric parameters. A more effective method to identify and discard spurious solutions is based on a measure of the radiated energy.

We define an energy radiation index (ERI) to be the total energy over a finite section of the guide in the far field, normalised by the total energy on the boundary of the truncated domain. For each geometry (for example radius of disc, separation between discs), truncation L and frequency k, an energy index is calculated over a section of the guide $R = R_- \cup R_+$, as shown in figure 1, with points $(x,y) \in R$ such $L - \lambda \leqslant |x| \leqslant L$, $-1 \leqslant y \leqslant 1$. Here λ is the usual wavelength $\lambda = 2\pi/k$. The energy radiation index is the ratio

$$\mathrm{ERI} = \frac{\int_{\mathrm{R}} \phi(x,y;k)^2\, dx\, dy}{\int_{\partial\Omega} \phi(x,y;k)^2\, ds}, \tag{3.4}$$

where ds is the arc length $ds^2 = dx^2 + dy^2$ and $\partial\Omega$ is the boundary of the truncated domain.

The ERI method of finding true or nearly trapped modes is implemented as follows: for a given geometry, truncation L and discretisation l, the values of k satisfying (2.10) are determined. For each such k, the eigenvector corresponding to the zero eigenvalue of the singular $M(k)$, provides a set of values for the unknowns, either ϕ or $\frac{\partial\phi}{\partial n}$, on each boundary element. These candidate numbers are substituted in (2.8) and $\phi(x,y;k)$ can be calculated and used to compute the energy radiation index using (3.4). For an exact solution, the radiation calculated sufficiently far from the trapping feature,

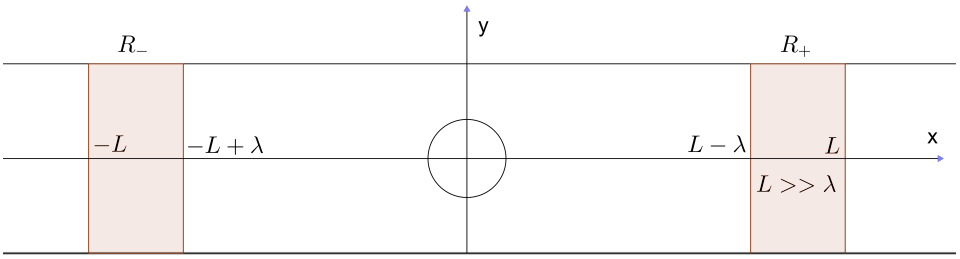

FIG. 1: The ERI estimates the total energy in $R = R_- \cup R_+$, normalised by energy on truncated domain boundary to provide a measure of the decay rate of the solution in the far field.

should be exponentially small. A mode obtained using the BEM method is an approximation of the exact solution and corresponds to a sharp local minimum in the space of parameters which define the domain's geometry. Typically, the geometrical parameter space is scanned fairly coarsely, and the corresponding k values are determined. The ERI is found for each case, and those values suggesting a local minimum are investigated more closely. The sharpness of the ERI minimum corresponding to a trapped mode is pronounced – a high ERI gradient invariably indicates at least a NTM in the vicinity. Occasionally, a non sharp local minimum is encountered which does not indicate a trapped mode. With experience, the trapped modes can be found quickly. Inevitably, if the initial scanning of parameter space is too coarse, modes may be missed, but in no case has our method failed to find a mode found by other authors.

This is a very effective method of distinguishing between real solutions and spurious L-dependent modes as the radiation indices can be compared for all values of k, in a given frequency range, corresponding to many sets of geometric parameters. Once a candidate k is found using the ERI method, other checks may be carried out to ensure the validity of results, which include the re-computation of the mode for finer resolution (l) and different waveguide truncations (L). For a genuine solution any changes in k, occurring due to these variations, should be no more than of order N^{-2}. As usual with eigenvalue calculations, an $O(\varepsilon)$ error in the eigenvector gives an $O(\varepsilon^2)$ error in the eigenvalue, so that the frequency k can be found accurately with a relatively coarse grid.

An example of the ERI method applied to the detection of an embedded mode for two sound-hard discs on the centreline of a Neumann guide now follows. The discs have equal radius a and their centres are separated by a distance c. The ERI is computed for sets (a,c) and all values of k such that $M(k)$ is singular. The data indicate at a glance which configurations are likely to support a trapped mode. Table 1 shows the lowest ERI for a range of (a,c) and $\pi/2 < k < 3\pi/2$. Note the final column is for $c = 4$ and was included to give an idea of the scale of variation.

The lowest ERI together with the corresponding k, are displayed for each (a,c). It can be seen that somewhere near the configuration $c = 2.8$, $a = 0.275$, the index has a sharp local minimum. (There is also the suggestion of a possible minimum near $(0.225, 2.9)$, but further data show that this is not the case.) A further indication that there are two competing modes can be seen from the k-values, which jump between $k \simeq 4.55$ and $k \simeq 4.5$ in the vicinity of the ERI minimum. The displayed frequencies in the immediate neigbourhood of a trapped mode candidate usually correspond to nearly trapped modes. The modes with higher radiation index are spurious.

Once parameter values corresponding to a (nearly) trapped mode are found, the solution can be

Energy Radiation Index					
	Separation c				
Radius a	2.6	2.7	2.8	2.9	4
0.225	0.031855	0.014048	0.002309	0.000939	0.012459
0.25	0.023881	0.009368	0.000987	0.001520	0.012049
0.275	0.012929	0.003928	$7.21E-05$	0.002299	0.010642
0.3	0.003989	0.000580	0.000372	0.003177	0.008521
0.325	0.001002	0.001419	0.002583	0.004141	0.005824
Corresponding k value					
	Separation c				
Radius a	2.6	2.7	2.8	2.9	4
0.225	4.5545	4.5523	4.5532	4.4542	4.5819
0.25	4.5551	4.5529	4.5538	4.4619	4.5867
0.275	4.5567	4.5546	4.4764	4.4715	4.4553
0.3	4.4782	4.4569	4.4946	4.4840	4.4679
0.325	4.4662	4.5278	4.5150	4.5006	4.4847

Table 1: Energy radiation index, and associated frequencies below the second cut-off ($\pi/2 < k < 3\pi/2$), for two discs in a Neumann guide. (a,c) are varied and the lowest ERI with the corresponding k are displayed. Note the 4th column is for $c = 4$, not $c = 3$. There is a sharp minimum near the middle of the data. The minimising k-values flit between two values, indicating two competing modes.

refined by scanning over intervals around the candidate geometric parameters. For example, the initial results in Table 1 are re-computed for $c \in [2.7, 2.9]$ and $a \in [0.25, 0.3]$ with increments 0.01 and the ERI minimum was found for $c = 2.84$, $a = 0.275$. This refining process can be repeated and the parameter values which give rise to real trapped modes established with increasing precision in a time-efficient manner. However, there is little point in exceeding the precision of the underlying grid.

In general, the accuracy of the scheme is limited by the discretisation (l,L). When a trapped mode is isolated in parameter space, a further error is introduced by the distance from the exact values. However, if we are close enough, this merely changes a trapped mode into a NTM, which is not critical in many applications. For a given discretisation and parameter set, the frequency can be obtained very accurately, but it will naturally differ from the exact trapped frequency because of the truncation. Below, we do not always refine the geometrical parameters to the maximum grid accuracy once it becomes clear that a NTM exists. When the trapped mode is part of a continuum, however. the k-values are automatically very accurate.

4. Discs on the centreline of a symmetric guide

For every $k \geqslant 0$, a travelling mode e^{ikx} satisfies the Neumann boundary condition on the waveguide. The continuous spectrum for this problem is $[0,\infty)$ Evans & Linton (1991), Jones (1953), hence all trapped modes are embedded. However, if the problem is restricted to finding only the $y-$antisymmetric solutions then the lower bound of the essential spectrum is $\pi/2$. With this restriction, the antisymmetric modes can be considered as non-embedded eigenvalues. For the case of one disc at the centre of an infinite Neumann guide it was established by Callan et al. (1991) that at least one trapped mode exists for all discs of radii $0 < a \leqslant 1$ below the first cut off $\pi/2$.

Evans & Porter (1997b) extended the work of Callan et al. (1991) constructing the solution for one disc on the centreline of a Neumann waveguide. They used a linear combination of suitably modified multipole potentials and sought trapped modes in the range $\pi/2 \leqslant k \leqslant 3\pi/2$. The existence of a second travelling mode in this frequency band required an extra constraint to ensure the corresponding propagating solution is zero at the trapped mode frequency. It was shown that only one value, $a = 0.352$ and a corresponding $k_c = 4.677 = 1.4896\pi$, satisfy the system of equations and the side condition simultaneously. Thus it is anticipated that in order to find trapped modes for higher frequencies it is necessary to consider obstacles defined by more parameters which could be varied. Placing the second disc at a variable distance from the first one provides such an additional geometric variable.

4.1 *Two identical discs in a Neumann guide*

The results obtained for the non-embedded modes are in agreement with those of Evans & Porter (1997a) for the case of a long narrow wave channel containing any number of different size bottom mounted circular cylinders arbitrarily spaced along the centreline of the channel. These modes correspond to acoustic resonances, where the same governing equations and boundary conditions apply. Evans and Porter have shown that there are no more than N trapped modes, in the range $0 < k < \pi$, for any configuration of N cylinders, the precise number depending critically on the geometry of the configuration. With $N = 2$, we extend these results for the next two bands of frequencies $\pi/2 < k < 3\pi/2$ and $3\pi/2 < k < 5\pi/2$.

The presence of a second disc provides an additional parameter, the spacing c, which for a given a, can be varied so that the amplitude of the additional travelling mode is zero at the trapped mode frequency. This rationale predicts that two discs will have more than one embedded trapped mode in this frequency range and that these should persist with the geometry, within certain limits. Indeed, using the BEM method, both symmetric and antisymmetric embedded modes are found in the range $\pi/2 < k < 3\pi/2$ for discs such that $0.1 \leqslant a \lesssim 0.4$ and discrete values of c. It is notable that the addition of another disc increases the maximum radius supporting an embedded mode above the value $a \approx 0.352$ for a single disc in the waveguide. A symmetric, embedded mode, for $a = 0.1$ and $c = 0.7112$, is presented in Fig. 2. Details of embedded modes found in this frequency range are given in Table 2. It is found that the antisymmetric modes decay slower with x and so require more numerical effort for the same accuracy. It can be seen from the table that the same disc size can support modes at more than separation distance. In figure (3), the symmetric and antisymmetric modes are drawn for $a = 0.2$.
The list provided is not exhaustive and further modes may be found for additional discrete values of the

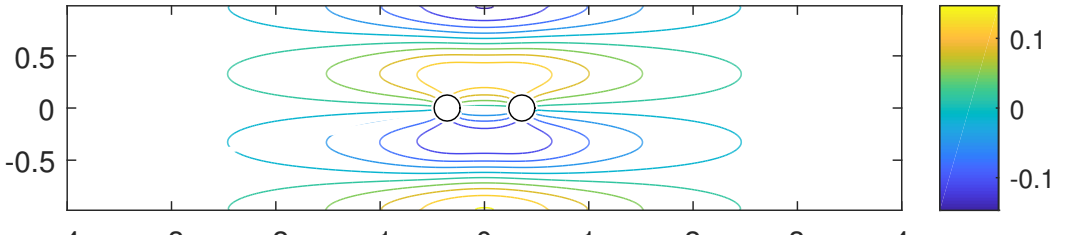

FIG. 2: Contours of ϕ for an embedded trapped mode for two discs of small radius $a = 0.1$ in a Neumann guide separated by $c = 0.7112$ for $k = 4.6746 \approx 1.4880\pi$.

spacing parameter c. Embedded modes are computationally harder to locate than non-embedded ones, as they are sensitive to minute changes in the geometry, appearing only for exact parameter values.

a	c	k	k/π	x-symmetry
0.10	0.7112	4.6734	1.4876	Symmetric
0.15	0.7336	4.5897	1.4610	Symmetric
0.20	0.7734	4.5291	1.4416	Symmetric
0.20	1.3666	4.6952	1.4945	Antisymmetric
0.25	0.7956	4.5404	1.4453	Symmetric
0.25	2.8948	4.6289	1.4734	Antisymmetric
0.25	1.4210	4.6915	1.4934	Antisymmetric
0.30	0.8934	4.5900	1.4611	Symmetric
0.35	1.3680	4.6803	1.4898	Symmetric
0.35	2.4632	4.6606	1.4835	Symmetric

Table 2: Embedded trapped modes for two identical discs in a Neumann guide.

Results above the second cut-off in the band $3\pi/2 < k < 5\pi/2$ are new, but follow a similar rationale e.g. to Porter & Evans (2005). The presence of three travelling modes in this frequency band suggests that only a single trapped mode may be possible for an exact combination of the geometric parameters a and c. Such a mode was found for $a = 0.18$, $c = 0.54$ for wavenumber $k \approx 7.72759 = 2.4597\pi$ and is shown in figure 4. It should be noted that accurate computations in this frequency range are expensive due to the high discretisation required to confirm a trapped mode. A NTM can be found more cheaply.

4.2 *Two discs of different radius in a Neumann guide*

Two discs of different radius $0 < a_1, a_2 \leqslant 0.8$, have either one or two modes in the range $0 < k < \pi/2$. Solutions corresponding to non-embedded frequencies are stable, in that varying the geometry does not destroy the trapped mode, it only continuously modifies the value of k. As the discs are different, the solutions do not display x-symmetry in the rigorous, mathematical sense. Instead we define quasi-symmetry for this configuration as follows: a mode may be either quasi-symmetric or quasi-antisymmetric if for a fixed y coordinate and large x, $\phi(x,y)$ and $\phi(-x,y)$ have identical or different signs respectively. Consider the case of two discs such that $a_1 < a_2$ with individual characteristic frequencies k_{c1}, k_{c2}. For overlapping discs one quasi-symmetric mode is found at a frequency k_s, near that corresponding to the larger disc, $k_s \approx k_{c2}$.

If one disc is large, $0.8 \leqslant a_1 \leqslant 1$ and the second is such that $0 < a_2 < 0.8$, the configuration has either two or three modes, depending on c. The case $a_1 = 0.9$ and $a_2 = 0.3$ is illustrated in Fig.5. The intersecting discs have two modes, one quasi-symmetric and one quasi-antisymmetric. As c increases a third mode appears - this particular geometry has a maximum of three trapped modes. For two larger discs, such $0.8 < a_1, a_2 \leqslant 1$, depending on c, this configuration has up to four trapped modes, two quasi-symmetric and two quasi-antisymmetric.

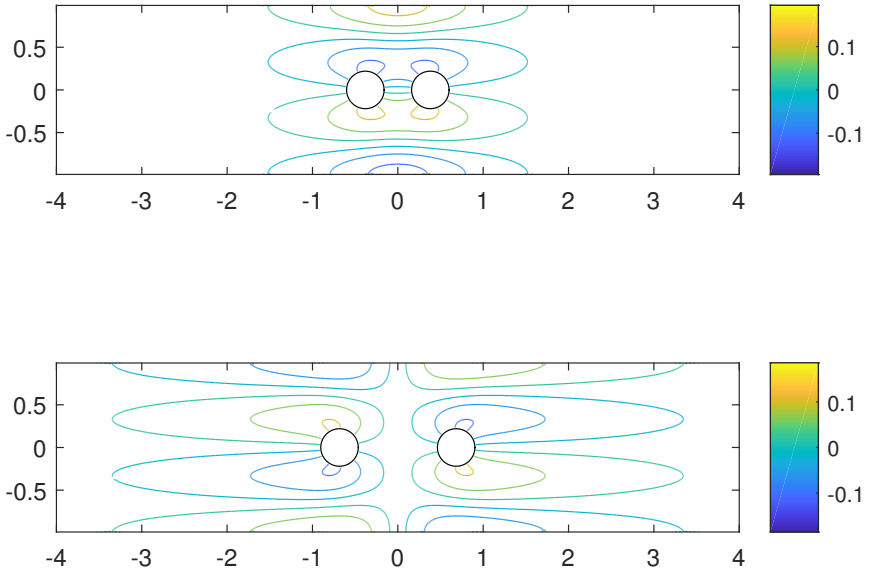

FIG. 3: Two embedded trapped modes for two discs of radius $a = 0.2$: one symmetric, at $c = 0.7734$ for $k = 4.5291 \approx 1.4416\pi$ and one antisymmetric at $c = 1.3666$ for $k = 4.6952 \approx 1.4945\pi$.

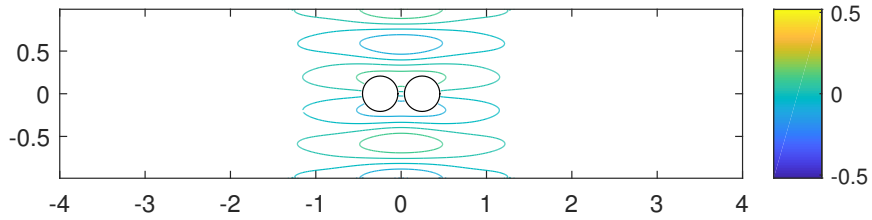

FIG. 4: Trapped mode embedded in $3\pi/2 < k < 5\pi/2$ for two discs of radius $a = 0.1775$, separation $c = 0.4911$ and $k = 7.7604 = 2.4702\pi$.

4.3 *Two identical discs in a Dirichlet guide*

The number and type of modes for two discs on the centreline of a Dirichlet waveguide were investigated up to the third cut-off. Two discs, of equal radius, $0 < a \leqslant 0.6$, on the centreline of a Dirichlet guide,

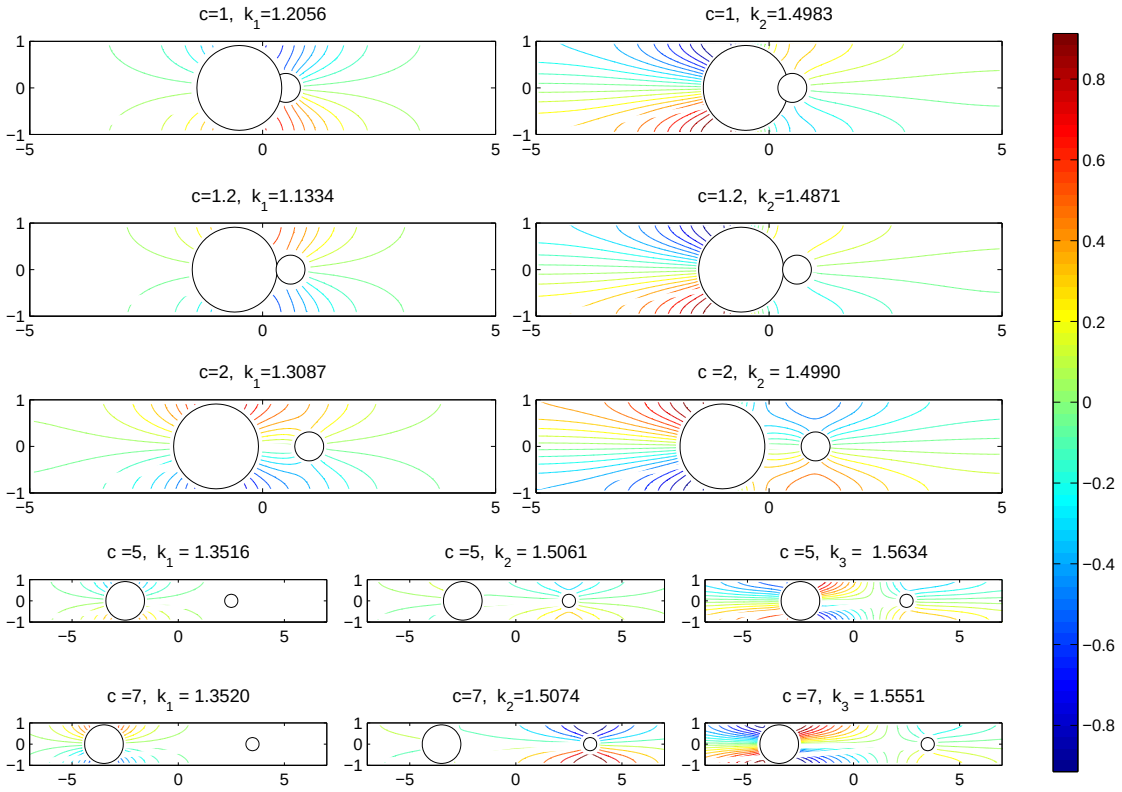

FIG. 5: Contours of multiple trapped modes for two discs $a_1 = 0.9, a_2 = 0.3$, in a Neumann guide, at the exact separation distances $c = 1$ (overlapping discs), $1.2, 2, 5$ and 7.

support one or two trapped modes, depending on the distance between them. The first, x-symmetric, mode can be found for any value of c, including overlapping discs. The second, x-antisymmetric, mode appears only for $c > 2a$. Frequencies for the symmetric and anti-symmetric modes are, in similar manner to the Neumann case, such that $k_s < k_c < k_a$. The results obtained for frequencies such that $\pi/2 < k < \pi$ are omitted as they are similar to those of Evans & Porter (1997a). We extend these results for the next frequency band $\pi < k < 2\pi$.

4.3.1 $\pi < k < 2\pi$ In this frequency range, only one embedded mode exists for a single disc on the centreline of a Dirichlet guide, for a specific value of a Linton & McIver (2007).

$$k \approx 6.258 = 1.992\pi, \; a = 0.267. \tag{4.1}$$

With two discs, for each k, the guide supports one propagating mode, but the additional parameter c can be varied until a trapped mode is found. Our results show that trapped modes exist for discs of all radii such that $0.1 \lesssim a \lesssim 0.3$ at discrete values of c. Some disc sizes were found to support more modes than others. For discs with $a = 0.125$ three trapped modes are possible whereas for a smaller discs, $a = 0.1$,

only one mode was found. The list of modes found for this geometry is given in Table 3. In Fig. 6(a) -

a	c	k	k/π	x-Symmetry
0.100	0.60	6.283	1.999	Symmetric
0.125	0.60	6.131	1.952	Symmetric
0.125	1.75	6.190	1.970	Symmetric
0.125	3.50	6.219	1.980	Antisymmetric
0.175	0.62	6.087	1.937	Symmetric
0.175	1.75	6.165	1.962	Symmetric
0.175	2.30	6.211	1.977	Antisymmetric
0.225	0.65	6.137	1.953	Symmetric
0.225	1.75	6.196	1.972	Symmetric
0.250	0.75	6.185	1.969	Symmetric
0.250	1.75	6.222	1.980	Symmetric
0.250	1.75	6.241	1.984	Symmetric
0.275	1.30	6.241	1.987	Symmetric
0.295	1.55	6.270	1.996	Symmetric

Table 3: Embedded trapped modes supported by two identical discs on the centreline of a Dirichlet guide.

6(c) we present three trapped modes for the same disc, with radius $a = 0.125$. The first plot, Fig. 6(a), corresponds to a small separation between discs $c = 0.6$. A second mode appears at a slightly larger separation, $c = 1.75$. Both these modes are symmetric in x and antisymmetric in y. As the distance increases, a third mode, anti-symmetric in both x and y, appears at $c = 3.35$.

It is possible that additional modes exist for increasing c and small values of a. The rationale for the last requirement is based on the fact that the high wavenumber gives rise to four potential peaks in the y-direction, as can be seen in Fig.6(a) - 6(c), which must be accommodated in the remaining space between the discs and the waveguide walls.

4.4 *Two discs of different radius in a Dirichlet guide*

In this section we present results for the case of two discs, with radii $a_1 = 0.2$, $a_2 = 0.5$, placed on the centreline of a soft guide. The discs have individual characteristic trapped mode frequencies, $k_{c1} = 3.0561 = 0.9728\pi$, $k_{c2} = 3.07145 = 0.9776\pi$. This type of geometry has either one or two trapped modes, depending on c. We use the terms quasi-symmetric and quasi-antisymmetric as defined in section 4.2. The modes are stable in the sense that frequencies vary continuously with c and they can be either quasi-symmetric or quasi-antisymmetric.

As c increases, three stages can be distinguished, as illustrated in Fig. 7. Firstly, for $0 < c < a_1 + a_2$ a single, quasi-symmetric, trapped mode exists for all c, with k decreasing almost linearly with c.

As $a_1 + a_2 \leqslant c \lesssim \lambda$ a second mode, quasi-antisymmetric appears at a higher frequency. The quasi-symmetric mode is coupled in the sense that there is interaction between the discs. The quasi-antisymmetric mode is decoupled, as exponential decay appears in the inner area and the interaction between discs is minimal.

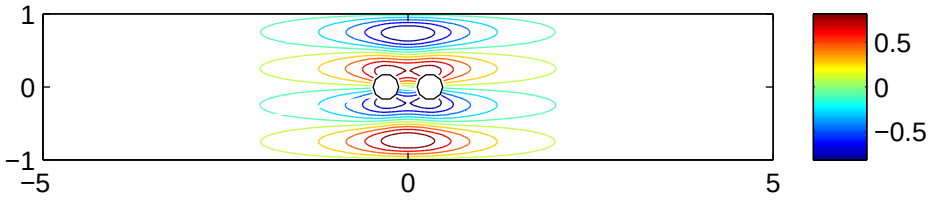

(a) $a = 0.125$, $c = 0.6$, $k \approx 6.1311 = 1.952\pi$.

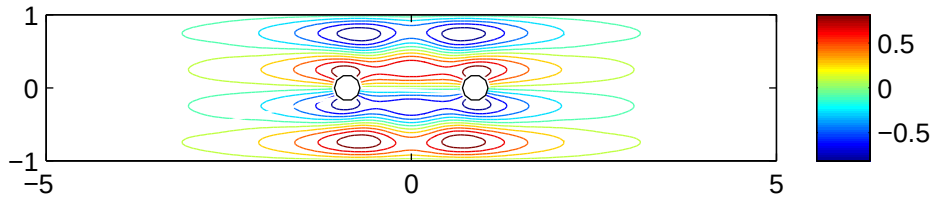

(b) $a = 0.125$, $c = 1.75$, $k \approx 6.190 = 1.970\pi$.

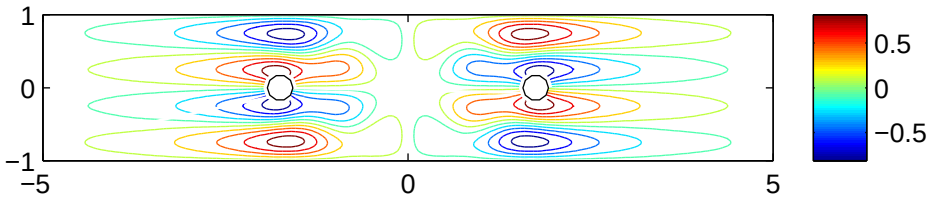

(c) $a = 0.125$, $c = 3.5$, $k \approx 6.219 = 1.980\pi$.

FIG. 6: Contour plots of three embedded modes, $\pi < k < 2\pi$, for two identical discs on the centreline of a Dirichlet guide.

As c increases above 3λ, the energy distribution between the two discs becomes skewed and the trapped mode becomes localised around one disc: the symmetric mode has a potential minimum/maximum on the boundary of the smaller disc, with $k_s < k_{c1}, k_s \to k_{c1}$ as $c \to \infty$. We also note that the quasi-antisymmetric mode has the highest amplitude oscillations on the boundary of the larger disc, with $k_a \to k_{c2}$ from above.

5. Waveguides with cavities

We now consider trapped modes in a guide which has a cavity on one wall. The simplest configuration is a rectangular cavity, consisting of a region of length $2w$ in which the guide width is increased from 2 to $2+h$.

5.1 *Rectangular cavity in a Dirichlet guide*

To begin with, we fix the cavity depth $h = 1$ and vary the width $2w$. Trapped modes are sought in the range $0 < k < \pi/2$. For narrow cavities, the solution decays slowly at infinity and the trapped mode

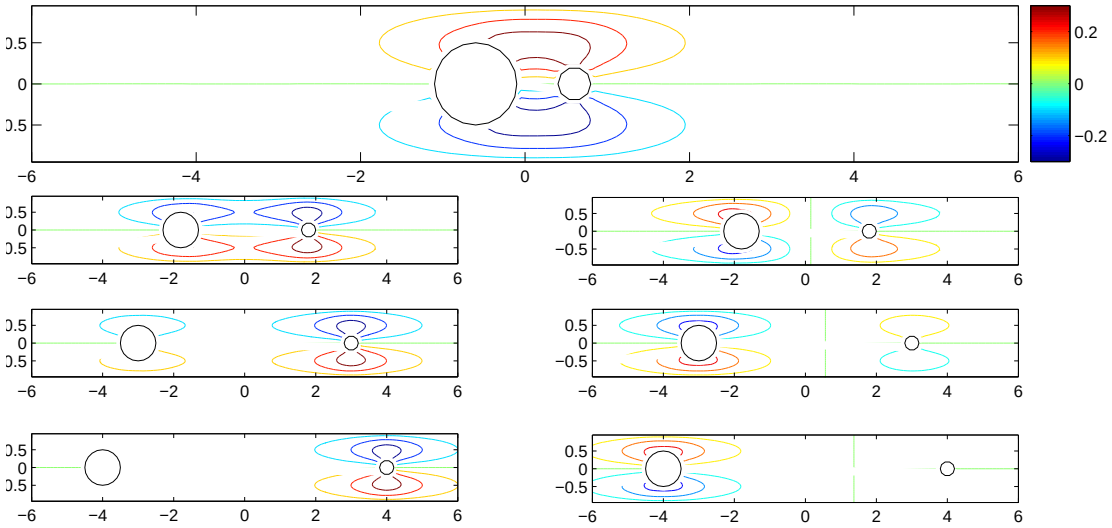

FIG. 7: Two discs, $a_1 = 0.2$, $a_2 = 0.5$, in a Dirichlet guide, for $c = 1.6$ (top) and $c = 3.6, 6$ and 8 (bottom). $c = 1.6$, $k \approx 2.987 = 0.951\pi$ (quasi-symmetric: QS), $c = 3.6$, $k = 3.055 \approx 0.973\pi$ (QS), $k \approx 3.087 = 0.983\pi$ (quasi-anti-symmetric: QA). $c = 6$, $k \approx 3.065 = 0.976\pi$ (QS), $k \approx 3.073 = 0.978\pi$ (QA). $c = 8$, $k \approx 3.066 = 0.976\pi$ (QS), $k = 3.071 = 0.978\pi$ (QA). Note the skewed distribution of ϕ between the two discs.

frequency is close to the cut-off value $\pi/2$. As $w \to 0$, the solution approaches the non-trapped standing wave solution $\phi \sim \cos\frac{\pi}{2}y$.

The following simple argument predicts the appearance of trapped modes. For generality, we consider both symmetric and anti-symmetric solutions with respect to the x-axis. The separable solutions in the waveguide far away from the cavity, takes the form

$$\phi = X(x)T(y) \sim \exp\left\{\pm i\left[k^2 - \left(\frac{\pi}{2}\right)^2\right]^{\frac{1}{2}} x\right\} \cos\left(\frac{\pi y}{2}\right). \tag{5.1}$$

Below the first cut-off, $k < \pi/2$, the y-symmetric oscillation cannot propagate down the guide. Now if w is assumed fairly large, in the region of the cavity around $x = 0$ we effectively have a wider guide, so that the Dirichlet condition on $y = 1$ and $y = -1-h$, suggests the y behaviour

$$Y(y) \approx \cos\left[\frac{\pi}{2}\left(\frac{y+h/2}{1+h/2}\right)\right] = \cos\left[\mu_2(y+h/2)\right], \tag{5.2}$$

with the x-dependence

$$X(x) \sim e^{\pm i\mu_1 x} \equiv \exp\left[\pm i\left(k^2 - \mu_2^2\right)^{\frac{1}{2}} x\right]. \tag{5.3}$$

Thus if k lies between the two cut-off values

$$\frac{\pi}{2+h} < k < \frac{\pi}{2}, \tag{5.4}$$

oscillations are possible in the cavity region, but not in the rest of the guide. A wave would effectively be trapped in the cavity. This is of course an over-simplification of the structure of the trapped mode. However, in the non-embedded regime, for this simple geometry, this argument renders the appearance of trapped modes plausible. Furthermore, applying the Dirichlet condition on the vertical cavity walls gives

$$\cos \mu_1 w = 0, \tag{5.5}$$

which together with (5.4), predicts that a trapped mode is possible below the first cut-off $k < \pi/2$ for a cavity of depth h and width $2w$ such that

$$w \gtrapprox \left(1 - \frac{1}{(1+h/2)^2}\right)^{-1/2}. \tag{5.6}$$

This predicts that for $h = 1$ if $w \gtrapprox 1.34$ y-even trapped modes are possible inside the cavity, but not down the guide. And indeed, using the BEM, it was found that an x-symmetric trapped mode exists for all cavities with $w \gtrapprox 1.35$. The approximation for k, depending on the cavity dimensions

$$k \approx \pi \sqrt{\left(\frac{1}{2+h}\right)^2 + \left(\frac{k_n}{\pi w}\right)^2}, \tag{5.7}$$

is also a useful indicator of the range of values which should be checked numerically in order to find the trapped mode frequency, saving significant computation time. In (5.7) $k_n = \pi/2, \pi, 3\pi/2, 2\pi, \ldots$ represent the guide cut-off values. For example, for a cavity of $h = 1, w = 2.7$, according to (5.7), a trapped mode should exist for $k \approx 1.1879 = 0.3781\pi$. The first trapped mode computed for this geometry has $k = 1.1524 \approx 0.3668\pi$. The estimate (5.7) predicts that k will decrease as the width of the cavity increases, which is consistent with the values found using the BEM. As the width of the cavity increases, additional, x-antisymmetric, modes appear for the same geometry, for new values of k which satisfy approximately $\mu_1 w = \pi$. As w increases, more trapped modes are found as new eigenvalues satisfy the condition

$$\mu_1 w = k_n. \tag{5.8}$$

Embedded modes, below the second cut-off $\pi/2 < k < \pi$, for this configuration exist only for discrete couples (h, w). The range $0 < h \leqslant 3, 0 < w \leqslant 3$ was investigated and the geometries found to support trapped modes, together with the relevant frequencies, are listed in Table 4. These modes have not previously been reported. To find these eigenvalues, boundary element steps of $l = 0.1$ and $l = 0.05$ were used, hence the spacing parameters h and w displayed in Table 4 have an expected error in the range $0.05 - 0.1$. A notable geometry is $h = 2.2, w = 2.9$ which supports two modes, at $k_1 \approx 2.7361 = 0.8709\,\pi$ and $k_2 \approx 3.03302 = 0.9654\,\pi$ (see Fig. 9(a) and 9(b)).

5.2 *Smooth cavity in a Dirichlet waveguide*

Whilst studying the trapped modes in rectangular cavities it was found that if the sharp corners at the top of the cavity were smoothed slightly, the trapped mode would disappear. This raised the question about the role of corner singularities in the formation of trapped modes and whether a smooth cavity would support trapped modes. Fernyhough (1998) demonstrate that this should not be the case, but

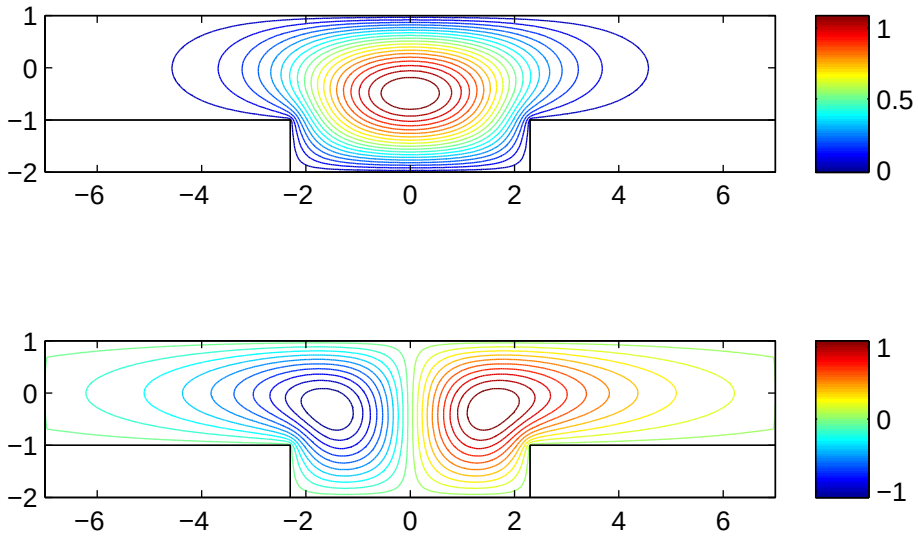

FIG. 8: Non-embedded trapped modes in a Dirichlet guide with a rectangular cavity of width $2w = 4.6$ and depth $h = 1$. $k \approx 1.1943 = 0.3801\pi$ (x-symmetric), $k \approx 1.5028 = 0.4783\pi$ (x-antisymmetric). Compare figure 3 of Wang (2014).

we nevertheless investigate a smooth cavity here. Let a Dirichlet waveguide have a lower boundary, prescribed by a Gaussian function

$$\Gamma_-(x) = -1 - he^{-(x/w)^2}. \tag{5.9}$$

Keeping one parameter fixed, e.g. $h = 1$, and varying w, it was found that non-embedded ($0 < k < \pi/2$) modes exist for all $w > 0.4$. The corresponding frequencies vary continuously with the geometry as illustrated in Fig. 10. Embedded modes in the higher frequency range, $\pi/2 < k < \pi$, exist only for discrete pairs (h,w). Two such modes are for $h = 3, w^2 = 1.8, k \approx 2.3442 = 0.7461\pi$ and $h = 2.6, w^2 = 0.8, k \approx 2.7473 = 0.8745\pi$. The first mode is plotted in Fig. 11.

5.3 *Triangular cavities in a Neumann waveguides*

A triangular indentation of maximum depth h and upper width w, supports trapped modes for discrete couples (h,w). These parameter values are similar to those which support trapped modes in rectangular cavities. Table 5 lists the modes found for this case. All modes found are even in x.

h	$2w$	k	k/π
2	3.8	2.482	0.790
2.2	5.8	2.731	0.871
2.2	5.8	3.033	0.965
2.6	2.8	2.902	0.924
3.0	3.4	2.657	0.846
3.0	3.9	2.621	0.834
2.1	5.2	2.373	0.755

Table 4: Embedded trapped modes supported by a rectangular cavity in a Dirichlet guide.

h	2w	k	k/π
2.9	7.6	1.456	0.464
3.5	10.4	1.245	0.396
3.9	11.6	1.159	0.369
5.6	8.8	1.349	0.429
5.9	9.6	1.282	0.408

Table 5: Trapped mode frequencies for a triangular cavity in a Neumann guide.

6. Rectangular cavity and disc on centreline of a waveguide

A single disc, of radius a, on the centreline of an infinite waveguide may support a trapped mode, depending on its size and the type of boundary condition on the guide. A cavity, of width w and depth h, in the absence of other obstacles in the guide, may support a trapped mode for discrete (h,w). Isolated thin or shallow cavities cannot support trapped modes – the spacing parameters must exceed some threshold in order for resonances to occur.

In general, the existence of travelling modes reduces the number of trapped modes. As the frequency is increased through each cut-off, for each new travelling mode an extra geometric constraint is required to ensure the corresponding propagating solution is zero at the trapped mode frequency Evans & Porter (1997b). Thus it is anticipated that geometries with more adjustable parameters will have a higher number of embedded frequencies. This rationale predicts that the combination of a disc and a cavity will have more than one embedded mode and that they should persist with the geometry, within certain limits. Indeed, it was found that the combination of a sound-hard disc aligned with a cavity greatly increases the affinity to trapped mode type resonances. For both the Dirichlet and the Neumann problem, trapped modes can be found for discs of all radii and for cavities of specific depth and width. The modes can be either x-symmetric or x-antisymmetric.

6.1 *Rectangular cavity and disc in the centre of a Neumann guide*

The problem was studied in the frequency range $0 < k < \pi/2$. Trapped modes can be found for a larger range of parameters than for a single disc or cavity as the combination of both gives rise to more

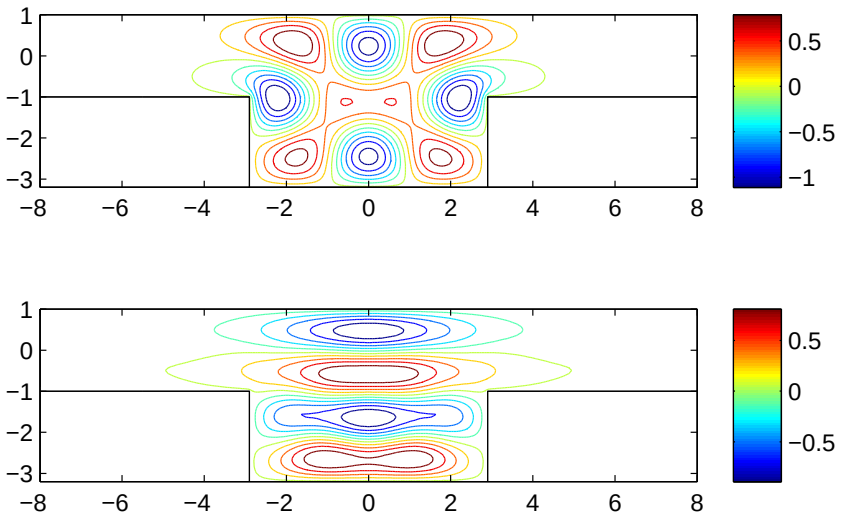

FIG. 9: Embedded trapped modes for the same rectangular cavity $2w = 5.8, h = 2.2$, in a Dirichlet guide. $k_1 \approx 2.7361 = 0.8709\,\pi$, $k_2 \approx 3.0330 = 0.9654\,\pi$.

resonances. For example, in the absence of a disc, shallow or narrow cavities do not support trapped modes. The minimum depth required for the appearance of a mode in a cavity is $h \gtrsim 2$, whereas the addition of a disc will enable trapped modes, in some cases, for cavities such that $h \approx 0.4$.

All discs of radius $0 < a \leqslant 1$, placed in the centre of the guide, support trapped modes for discrete couples of (h,w). A disc of a given radius supports trapped modes for more than one cavity, for discrete, specific couples (h,w). The case $a = 1$ is included because a cavity of width $w > 1$ allows the whole domain to remain connected.

The addition of a disc enables the appearance of trapped modes in the presence of cavities which otherwise would not support trapped modes. For a given cavity depth it is possible that there are no trapped modes, irrespective of its width and the disc radius. Some cavities may support modes in conjunction with more than one disc. For example, a guide with a cavity of depth $h = 4.6$ and $2w = 4.2$, has an x-symmetric trapped mode for disc of radius $a = 0.3$ and a different, x-antisymmetric mode, for $a = 1$. For nearby values of a, the trapped mode is perturbed, giving rise to nearly trapped modes with low radiation, which physically would be difficult to distinguish from the trapped mode itself. Table 6 shows trapped mode frequencies for the fixed $a = 0.4$ and cavities in the range $h \in (0,6), 2w \in (0,7)$ The k values found vary noticeably from case to case in contrast to those for an isolated disc in the waveguide, which are close to the relevant cut-off. The plots illustrate the evolution of the trapped modes as the cavity size increases. As the horizontal walls of the cavity are pulled further apart, the solution develops new local critical points on the cavity walls, at $x = \pm w$ (see Fig. 14). As the cavity increases further, an antisymmetric mode appears, with a series of peaks and troughs on the cavity walls (see Fig. 15).

FIG. 10: Trapped mode frequencies below the first cut-off, $0 < k < \pi/2$, for a Gaussian cavity in an infinite Dirichlet guide.

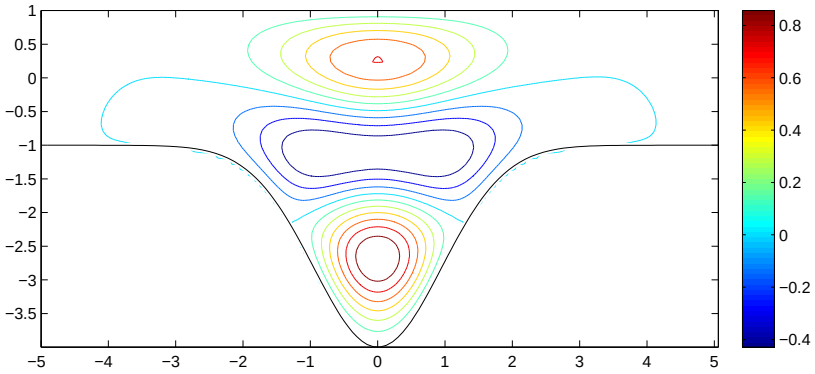

FIG. 11: Embedded trapped mode in a smooth cavity with Gaussian profile, $h = 3, w^2 = 1.8$ and frequency $k \approx 2.3442 = 0.7461\pi$.

6.2 *Rectangular cavity and disc in a Dirichlet waveguide*

The combination of the two aligned features, cavity and disc, greatly increases the number of trapped mode resonances, and the resultant spectrum may provide information about the nature of the wall

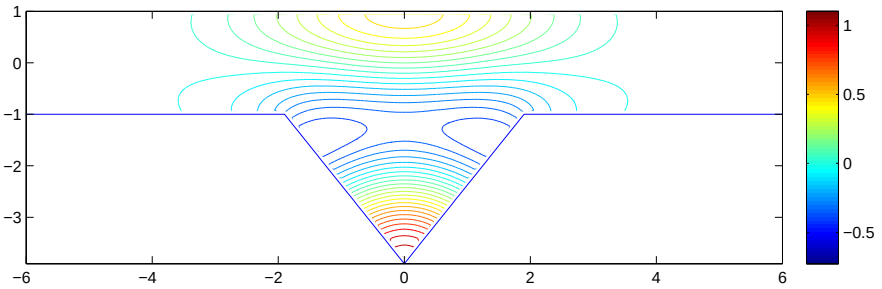

FIG. 12: An embedded trapped mode in a triangular cavity, $h = 2.9, w = 3.8$ and frequency $k \approx 1.4563 = 0.4635\pi$.

h	$2w$	k	k/π	x-Symmetry
0.8	6.0	1.157	0.368	Symmetric
1.4	6.75	0.988	0.315	Symmetric
1.0	7.0	1.264	0.402	Antisymmetric
3.4	6.0	1.147	0.365	Symmetric
3.8	6.2	1.095	0.348	Symmetric
4.8	4.4	1.362	0.433	Symmetric (see Fig 13)
4.2	7.0	1.025	0.326	Symmetric
4.6	3.4	1.402	0.446	Symmetric (see Fig. 14)
4.95	6.6	1.456	0.463	Antisymmetric (see Fig. 15)

Table 6: Trapped mode frequencies for a cavity and a sound hard disc at the centre of a Neumann guide.

cavity. For a single cavity, six modes were found in the range $0 < h \leqslant 6$, $0 < w \leqslant 6$ (Table 4). With the addition of a disc, for the same cavity parameters, the number of trapped modes increased to 84. The list of trapped mode frequencies found for this structure and a selection of plots to illustrate the variety of solution found are included in Appendix A. The modes are presented in increasing order of cavity depth.

Any disc of radius $0 < a \leqslant 1$, placed at the centre of a Dirichlet guide, supports trapped modes for one or more discrete couples (h,w). It is notable that the presence of a cavity extends the radius for which trapped modes are possible above the $a = 0.67$ limit found for an isolated disc (Callan et al. (1991), Maniar & Newman (1997)).

For a given cavity it is possible that there are no trapped modes, irrespective of the disc radius. However, the trapped mode (a,h,w) triples are densely distributed therefore most geometries are likely to support at least a nearly trapped mode. It is therefore possible, to find either a trapped mode or a nearly trapped mode with low radiation, for any given $0 < a \leqslant 1$ and most values of h and w. Although not

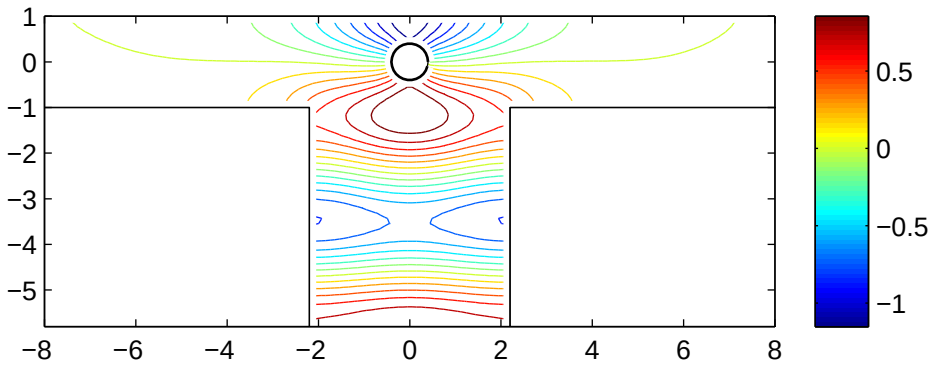

FIG. 13: Trapped mode for a rectangular cavity and a disc at the centre of a Neumann guide, $h = 4.8, w = 4.4$ and frequency $k \approx 1.3615 = 0.4334\pi$.

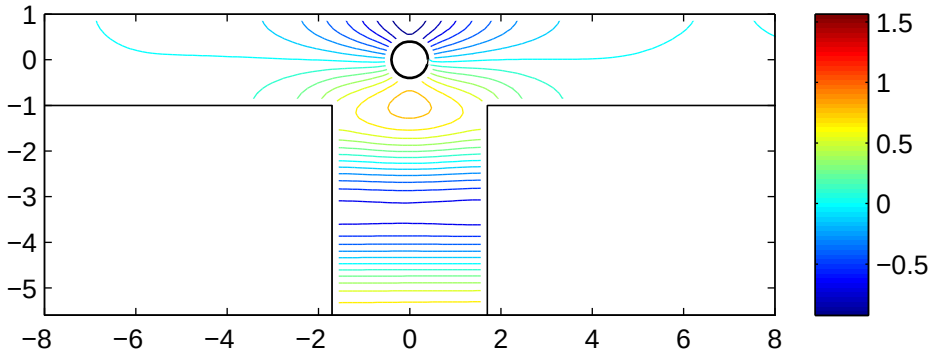

FIG. 14: Trapped mode for a rectangular cavity and a disc on centre of a Neumann guide, $h = 4.6, 2w = 3.4$ and frequency $k \approx 1.4024 = 0.4464\pi$.

an exact solution to the problem, nearly trapped modes would physically be very difficult to distinguish from the perfectly decaying modes.

Some configurations may support more than one mode. Two cases were identified within the parameters studied $(0 < a \leqslant 1, 0 < h \leqslant 6, 0 < w \leqslant 6)$, where the same structure has two trapped modes, at two

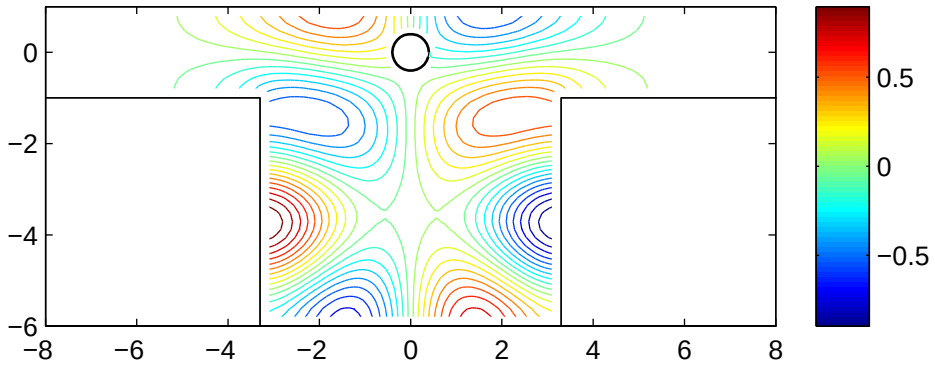

FIG. 15: Trapped mode for a rectangular cavity and a disc at the centre of a Neumann guide, $h = 4.95, 2w = 6.6$ and frequency $k \approx 1.4557 = 0.4634\pi$.

different frequencies. Plots for these cases can be found in Appendix A.

6.3 *Rectangular cavity and off-centre disc in a Neumann and a Dirichlet guide*

Finally, geometries without any x or y-symmetry, were considered for both Dirichlet and Neumann guides, with a sound-hard disc and a rectangular cavity. The removal of the disc from the centre of the guide, even by a small distance, so that $0 < x_c \ll 1$, leads to the disappearance of the trapped mode. In most cases a small perturbation gives rise to a nearly trapped mode. As the distance x_c is increased, nearly trapped modes also disappear. As $x_c \gtrsim \lambda$, a wavelength, a nearly trapped mode, corresponding to the pure trapped mode for either a single cavity or a single disc, is recovered. This occurs at frequencies similar but not identical to those corresponding to pure trapped modes. These modes are localised either around the disc or the cavity. The mode formed around the disc is perturbed in the region and beyond the cavity. Also, the mode trapped by the cavity is perturbed around and beyond the disc. An illustration of this behaviour, in a Dirichlet guide, where the disc is removed from the centre to $x_c = -6$, is presented in Fig. 16(a) -16(b).

No pure trapped modes were found for any asymmetric geometry, irrespective of the disc radius and cavity size. This does not exclude the possibility that a trapped mode may exist for a specific set of values (a, h, w, x_c), however such a geometry was not identified.

7. Nearly trapped modes

Nearly trapped modes (NTMs) appear consistently throughout this problem. Unlike pure trapped modes, which are characterised by zero radiation, nearly trapped modes are near-resonances with small radiation. The BEM developed is therefore ideally suited for their detection. Although NTMs are not a solution in that they do not satisfy the decay condition in the far field, they are important because of the physical, practical implications. The high amount of energy present in the near field, in comparison with the amount that radiates, is important in predicting the forces on the trapping features.

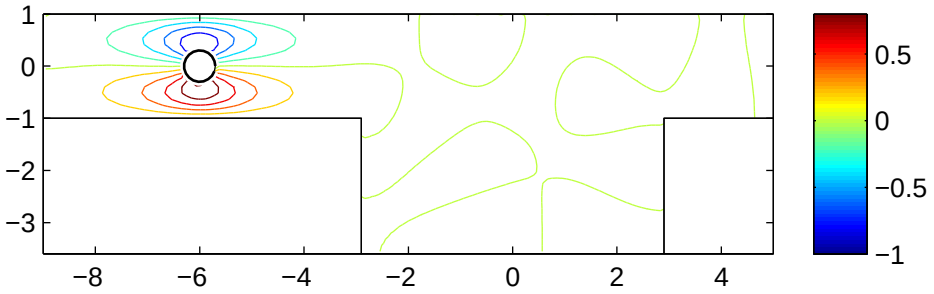

(a) Nearly trapped mode at $k \approx 2.9931 = 0.9527\pi$. Without the cavity, the trapped frequency is $k_c \approx 2.9907 = 0.9511\pi$

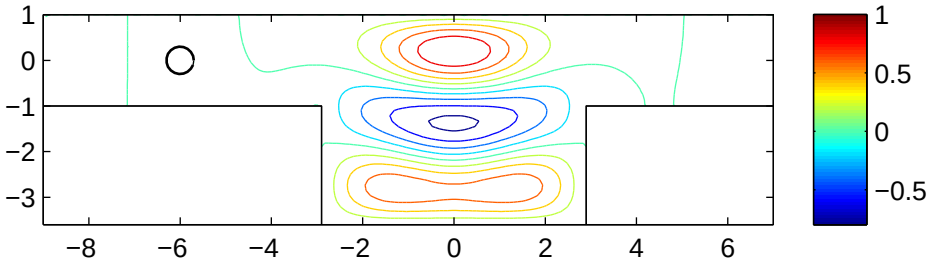

(b) Nearly trapped mode at $k \approx 2.7037 = 0.8606\pi$. Without the disc the trapped frequency is $k_c \approx 2.6566 = 0.7900\pi$

FIG. 16: Nearly trapped modes in a Dirichlet guide with a rectangular cavity $h = 2.6$, $w = 5.8$ and a disc of radius $a = 0.3$ over a wavelength away, $x_c \gg \lambda$. Two NTMs resemble the trapped modes ignoring either the cavity or disc.

There are two main categories of nearly trapped modes which were found numerically: 1) perturbations of exact trapped modes 2) modes with low radiation which are not related to any trapped modes.

The specific set of parameters corresponding to an embedded trapped mode is a discrete point in a continuous band of parameters which all support nearly trapped modes. As a result a geometry which approximates that required for a trapped mode will give rise to a nearly trapped mode which in a physical system might be indistinguishable from an exact resonant mode. This is illustrated by the data in Table 1 referring to the Neumann waveguide with two sound-hard discs for which a and c are uniformly varied. The energy radiation sharply decreases as the configuration approaches that required for the formation of a trapped mode but it can be seen that slightly perturbed configurations have low energy loss, corresponding to a nearly trapped mode. These NTMs are important as some of the geometric specifications for trapped modes are idealised and not likely to occur in physical situations. Physical systems which closely approximate those required for a trapped mode are then likely to give rise to the related, nearly trapped modes. For example, an infinite or doubly infinite periodic array of vertical cylinders is known to support pure trapped waves. In finite arrays near-trapping occurs in the form of large resonances which appear at the incident wave frequency which corresponds to the trapped mode frequency for the infinite array Evans & Porter (1999). Maniar & Newman (1997) calculated the distribution of forces along a finite array of 100 cylinders at the 'near-trapping' frequency and shown that the force on the middle cylinder is approximately 34 times higher than that on an isolated cylinder.

The second category discovered is that of NTMs which are not related to any trapped modes at real frequencies. For example two large discs $0.6 < a \leqslant 1$ in a Dirichlet guide were found to support only nearly trapped modes. They are y-symmetric, whereas all the trapped modes found for smaller discs are y-antisymmetric. The amplitude in the inner area is about 100 times higher than in the outer area. The disc radii and separation c can be varied continuously and the radiation index remains approximately constant. These modes exist for all c above a certain threshold. For larger separations more than one mode can be found for the same geometry and they can be either symmetric or antisymmetric in x. An example of such a mode, for $a_1 = a_2 = 0.7$, is presented in Fig. 17.

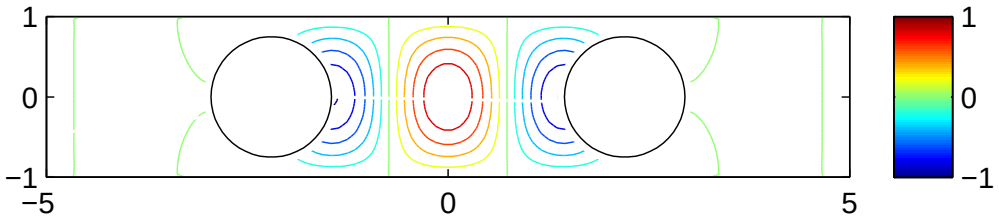

FIG. 17: An x and y-symmetric nearly trapped mode, $a = 0.7$, $c = 4.4$ and $k \approx 2.6497 = 0.8434$. The potential is not zero in the far field, there is 10^2 difference in amplitude between the inner and outer areas.

8. Summary and concluding remarks

A robust and efficient boundary element program for the detection of trapped modes in both bounded and unbounded 2-D domains has been used to confirm and extend existing results for sound-hard circular discs in both Neumann and Dirichlet waveguides with or without cavities.

An effective strategy, based on the combination of a decaying boundary condition and an estimate of the radiation in the far field (ERI), was devised to locate genuine and nearly trapped modes and to discard spurious modes which appear due to domain truncation. The ERI method is a useful measure of the energy leak associated with nearly trapped modes which are of practical importance. The presence of NTMs is in general an indication of nearby configurations which support a pure trapped mode.

Known results for two sound-hard discs of radius a in Neumann and Dirichlet guides were extended. Embedded modes were found for discrete values of the distance between discs and any $a \leqslant 0.4$ for Neumann guides and $a \leqslant 0.3$, for Dirichlet guides. The numerical scheme developed is also used to investigate the related topic of nearly trapped modes.

Wall cavities of sufficient size were found to give rise to various numbers of trapped modes in a predictable manner. It was found that a soft guide with a rectangular cavity has embedded modes $(\pi/2 < k < \pi)$ for discrete couples (h, w). In the parameter range $0 < h \leqslant 6$, $0 < 2w \leqslant 6$, seven trapped modes were found. Notably, two different x-symmetric trapped modes, at two different frequencies, were found for $h = 2.2, 2w = 5.8$.

Ir was shown that cavities without corner singularities can give rise to trapped modes, by investigat-

ing a Dirichlet guide with a smooth Gaussian lower boundary. Non-embedded trapped modes exist for all such cavities above a certain size and their k-values vary continuously with the geometry. Embedded modes in the next frequency range $\pi/2 < k \leqslant \pi$, exist only for discrete pairs (h,w). Undoubtedly more embedded modes could be found if the number of geometric parameters defining the boundary were increased.

Triangular cavities, in a Neumann guide, with $0 < h \leqslant 6$, $0 < 2w \leqslant 6$, were investigated and five embedded modes were found. These results suggest that any large symmetric cavity in either a Dirichlet or Neumann guide, would support embedded trapped modes, below the second cut-off, for specific couples (h,w).

The complexity increases when there is both an inclusion and a cavity. A sound-hard disc on the horizontal centreline of a guide with a rectangular cavity exhibits trapped modes for discrete triples (a,h,w) in both Neumann and Dirchlet cases. It was established that discs of all radii $(0 < a \leqslant 1)$ support trapped modes for many associated cavities. This contrasts with the case of a single disc in a Dirichlet guide in the absence of a cavity, which has one trapped mode in the range $\pi/2 < k < \pi$, but only if $0 < a < 0.67$. The presence of the disc also extends the range of cavities which support trapped modes, as in general thin or shallow cavities do not support embedded trapped modes. Thus the cavity may be detected by the sudden appearance of a trapped mode as the disc moves down the channel. If the geometry is constrained too much it is not always possible to find a trapped mode, so that for a given rectangle (h,w), there may not exist a trapped mode irrespective of the disc's size. As usual with embedded modes, perturbing a geometric parameter formally destroys the trapped mode. However, for this geometry many nearly trapped modes were found, some with low radiation, so that physically they would be difficult to distinguish from genuine trapped modes.

Geometries without any (x,y) symmetry were also considered. As the disc is removed from the cavity's vertical symmetry line, any existing trapped mode is destroyed. No pure trapped modes were discovered for asymmetric geometries, irrespective of the disc radius and cavity size. This does not exclude the possibility that a trapped mode may exist for a specific set of values (a,h,w,x_c,y_c), but no such geometry was found. If the disc is moved more than one wavelength away from the cavity, nearly trapped modes, corresponding to the pure modes of either the isolated disc or cavity, appear. These modes are localised around either the disc or the cavity, decaying away from the trapping feature and perturbed near the cavity or disc, respectively. The frequencies are similar but not identical to those corresponding to the pure trapped modes in the absence of cavity or disc.

In summary, for the cases we have studied, at least one symmetry line seemed necessary for genuine trapped mode resonances (but see Nazarov (2013)). Increasing the number of trapping features, placed with a degree of symmetry, leads to the appearance of new trapped modes. The addition of a new geometric parameter to a problem which has one embedded trapped mode solution for a specific discrete geometry, leads to the appearance of a continuum of trapped modes.

Applications of trapped mode studies fall into three broad categories: first, the situations where trapped modes are undesirable. Embedded modes especially may be excited by travelling waves of the same frequency by nonlinear processes leading to the accumulation of energy with destructive effects on a structure. Examples are constructions supported by large arrays of standing columns (offshore platforms, bridges and proposed designs for floating airports), long tunnels for high speed trains and cavities in quantum waveguides, with application to particle accelerators Caspers & Scholz (1996).

The second category relates to obtaining information about structures which are not directly accessible. Trapped modes are suitable for these applications due to their high localisation and the fact that they are sensitive to environmental changes. A growing body of research is concerned with their use for sensors and non-destructive testing. A fraction of the energy of a travelling wave excites the (nearly)

trapped mode through mode conversion which then leaks out Cobelli et al. (2011). This leak appears as a long-tailed ringing due to a high quality factor (Q) of the trapped mode Onoe (2007). Extensive experiments have been conducted Onoe & Suzuki (2007) to assess the feasibility of remote excitation of trapped energy modes in plates and pipes and its applications to sensors and non-destructive testing.

A third category is that of structures where high resonance at a narrow band of frequencies is desired. For example achieving resonances with high-Q factors is essential in order to make the performance of metamaterials more efficient. As recent theoretical analysis showed, high-Q resonances involving trapped modes are possible in metamaterials. Fedotov et al. (2007) reported exceptionally narrow transmission and reflection resonances in planar metamaterials. The appearance of the narrow resonances is attributed to the excitation of, otherwise inaccessible, symmetric trapped modes.

The rich catalogue of results obtained leads us to conclude that even for systems where exact trapped modes may be fairly rare occurrences, nearly trapped modes are widespread and of practical importance.

Acknowledgment

This work was funded by the Engineering and Physical Sciences Research Council and the Defence Science and Technology Laboratory.

REFERENCES

Brebbia, C. A., Faria, T. J. C. & Wrobel, L. C. (1984) *Boundary element techniques: theory and applications in engineering*. Springer-Verlag, Berlin and New York.

Callan, M. A., Linton, C. M. & Evans, D. V. (1991) Trapped modes in two-dimensional waveguides. *J. Fluid Mech.*, **229**, 51–64.

Carini, J. P., Londergan, J. T., Mullen, K. & Murdock, D. P. (1992) Bound states and resonances in waveguides and quantum wires. *Phys. Rev. B*, **46(23)**, 15538 – 15541.

Caspers, F. & Scholz, T. (1996) Measurement of trapped modes in perforated waveguides. *Particle accelerators*, **51**, 251–262.

Chen, J. T., Wu, C. F., Chen, I. L. & Lee, J. W. (2012) On near-trapped modes and fictitious frequencies for water wave problems containing an array of circular cylinders using a null-field integral equation. *Eur. J. Mech. B/Fluids*, **32**, 32–44.

Cobelli, P. J., Pagneux, V., Maurel, A. & Petijeans, P. (2011) Experimental study on water-wave trapped modes. *J. Fluid Mech.*, **666**, 445–476.

Duan, Y., Koch, W., Linton, C. M. & McIver, M. (2007) Complex resonances and trapped modes in ducted domains. *J. Fluid Mech.*, **571**, 119–147.

Evans, D. V., Levitin, M. & Vassiliev, D. (1994) Existence theorems for trapped modes. *J. Fluid Mech.*, **261**, 21–31.

Evans, D. V. & Linton, C. M. (1991) Trapped modes in open channels. *IMA J. Appl. Maths*, **49**, 45–60.

Evans, D. V., Linton, C. M. & Ursell, F. (1993) Trapped mode frequencies embedded in the continuous spectrum. *Q. J. Mech. Appl. Math*, **46(2)**, 253–274.

Evans, D. V. & Porter, R. (1997a) Trapped modes about multiple cylinders in a channel. *J. Fluid Mech.*, **339**, 331–356.

Evans, D. V. & Porter, R. (1997b) Trapped modes embedded in the continuous spectrum. *Q. J. Mech. Appl. Math*, **51**, 263–274.

Evans, D. V. & Porter, R. (1999) Trapping and near-trapping by arrays of cylinders in waves. *Journal of Engineering Mathematics*, **35**, 149–179.

Exner, P. & Seba, P. (1989) Bound states in curved quantum waveguides. *J. Math. Phys*, **30(11)**, 25742580.

Fedotov, V. A., Rose, M., Prosvirnin, S. L., Papasimakis, N. & Zheludev, N. I. (2007) Sharp Trapped-Mode Resonances in Planar Metamaterials with a Broken Structural Symmetry. *Phys. Rev. Lett.*, **99**, 147401.

Fernyhough, M. (1998) Full multimodal analysis of an open rectangular groove waveguide. *IEEE Trans. Microwave Theory Tech.*, **46**, 97–107.

Hein, S. & Koch, W. (2008) Acoustic resonances and trapped modes in pipes and tunnels. *J. Fluid Mech.*, **605**, 401–428.

Hohage, T. & Nannen, L. (2015) Convergence of infinite element elements for scalar waveguide problems. *BIT Num. Math.*, **55**, 215–254.

John, F. (1950) On the motion of floating bodies. *Commun. Pure Appl. Math*, **3**, 45–10.

Jones, D. S. (1953) The eigenvalues of $\nabla^2 u + \lambda u = 0$ when the boundary conditions are given in semi-infinite domains. *Proc. Camb. Phil. Soc*, **49**, 668–684.

Kuznetsov, N., Maz'ya, V. & Vainberg, B. (2002) *Linear Water Waves*. Cambridge University Press, Cambridge.

Linton, C. M. (1998) The Green's function for the two-dimensional Helmholtz equation in periodic domains. *J. Eng. Maths*, **33**, 377–401.

Linton, C. M. & McIver, P. (2007) Embedded trapped modes in water waves and acoustics. *Wave Motion*, **45**, 16–29.

Maniar, H. D. & Newman, J. N. (1997) Wave diffraction by a long array of cylinders. *J. Fluid Mech.*, **339**, 309–330.

McIver, M. & Linton, C. M. (1995) Acoustic Wave Trapping in One-Dimensional Axisymmetric Arrays. *Q J Mechanics Appl Math.*, **48 (4)**, 543–555.

McIver, M., Linton, C. M., McIver, P., Zhang, J. & Porter, R. (2001) Embedded trapped modes for obstacles in two-dimensional waveguides. *Q. J. Mech. Appl. Math.*, **54**, 273–293.

Nazarov, S. A. (2013) Enforced stability of a simple eigenvalue in the continuous spectrum of a waveguide. *Func. Anal. Appl.*, **47**, 195–209.

Onoe, M. (2007) Remote excitation of trapped energy modes in plates and pipes and its applications to sensors and NDT. *Proc. Frequency Control Symp.*, **15**, 488–793.

Onoe, M. & Suzuki, T. (2007) Experimental study on remote excitation of trapped energy modes of vibration. *Proc. Symp. Ultrasonic Electronics*, **20**, 3–9.

Pendry, J. B. (2000) Negative Refraction makes a perfect lens. *Phys Rev Lett.*, **85**, 3966–3969.

Pendry, J. B. (2004) Negative refraction. *Contemporary Physics*, **45**, 191–202.

Podolskiy, V. A., Sarychev, A. K. & Shalaev, V. M. (2003) Plasmon modes and negative refraction in metal nanowire composites. *Optics Express*, **11(7)**, 735–745.

Porter, R. & Evans, D. V. (2005) Embedded Rayleigh - Bloch surface waves along periodic rectangular arrays. *Wave Motion*, **43**, 29–50.

Postnova, J. & Craster, R. V. (2008) Trapped modes in elastic plates, ocean and quantum waveguides. *Wave Motion*, **45 (4)**, 565–579.

Sargent, C. V. (2012) *Trapped modes of the Helmholtz equation*. PhD thesis, Imperial College, London.

Simon, M. J. & Ursell, F. (1984) Uniqueness in linearized two-dimensional water-wave problems. *J. Fluid Mech.*, **148**, 137–154.

Ursell, F. (1951) Trapping modes in the theory of surface waves. *Proc. Camb. Phil. Soc*, **47**, 347–358.

Wang, C. Y. (2014) Effect of local enlargement on the trapped modes of infinite or semo-infinite membrane strips. *Mech. Res. Comm*, **57**, 6–9.

A. Multiple modes for a disc and rectangular cavity in a Dirichlet guide

a = 0.2

Mode No.	h	w	k	k/π	Type
0.2 - 1	2.0	1.2	3.05274	0.97172	Symmetric
0.2 - 2	2.4	2.9	2.94200	0.93647	Symmetric
0.2 - 3	2.7	1.7	2.83115	0.90118	Symmetric
0.2 - 4	3.6	2.9	2.94046	0.93598	Symmetric
0.2 - 5	3.7	3.6	2.83115	0.90118	Symmetric
0.2 - 6	4.0	1.2	3.05436	0.97223	Symmetric
0.2 - 7	4.0	3.5	2.71868	0.86538	Symmetric

Mode No 0.2 - 1

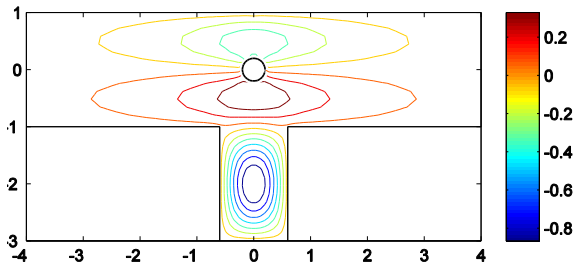

Mode 0.2 - 6

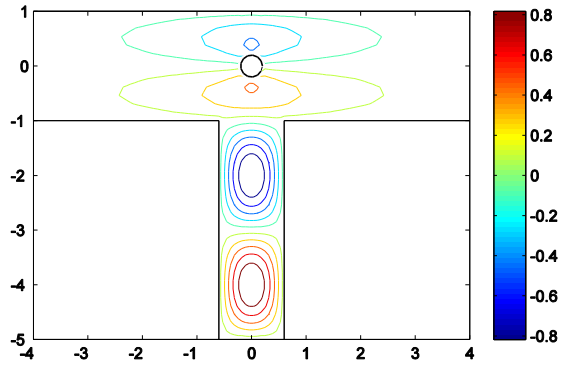

Mode No. 0.2 - 5

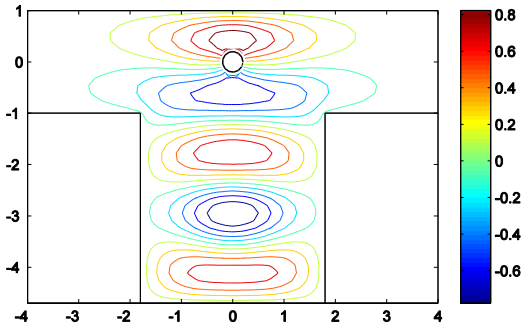

Mode No. 0.2 - 7

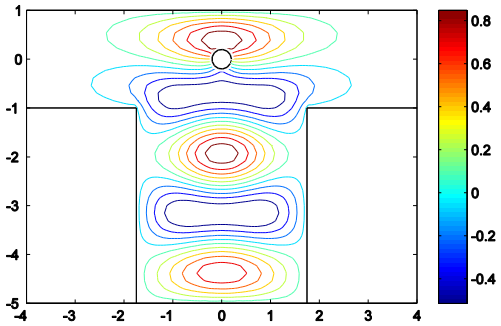

a= 0.3

Mode No.	h	w	k	k/π	Type
0.3 - 1	1.2	3.4	2.91233	0.92702	Symmetric
0.3 - 2	1.6	4.0	2.64178	0.84090	Symmetric
0.3 - 3	1.6	3.4	3.04218	0.96836	Antisymmetric
0.3 - 4	1.8	1.3	2.98267	0.94941	Symmetric
0.3 - 5	2.6	1.8	2.98330	0.94961	Symmetric
0.3 - 6	2.2	3.4	2.99660	0.95385	Symmetric
0.3 - 7	2.8	1.6	2.99660	0.95385	Symmetric
0.3 - 8	2.8	3.2	3.07459	0.97867	Antisymmetric
0.3 - 9	3	3.8	2.59016	0.82447	Symmetric
0.3 - 10	3	3.6	2.96646	0.94425	Antisymmetric
0.3 - 11	3.2	3.2	3.06215	0.97471	Symmetric
0.3 - 12	3.2	4.2	3.01957	0.96116	Symmetric
0.3 - 13	3.2	4	2.81968	0.89753	Antisymmetric
0.3 - 14	3.2	4	3.02608	0.96323	Symmetric
0.3 - 15	3.2	4.2	3.01957	0.96116	Symmetric
0.3 - 16	3.2	5	2.69225	0.85697	Antisymmetric
0.3 - 17	3.8	4.8	2.49856	0.79532	Antisymmetric
0.3 - 18	4.2	1.6	2.98325	0.94960	Symmetric

Mode No. 0.3 – 2

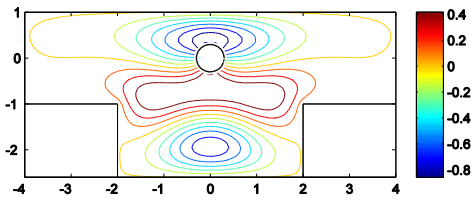

Mode No. 0.3 – 3

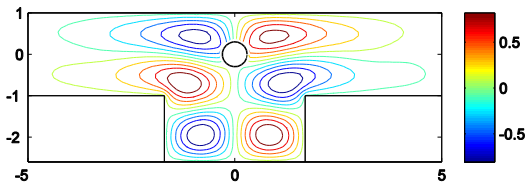

Mode No. 0.3 – 5

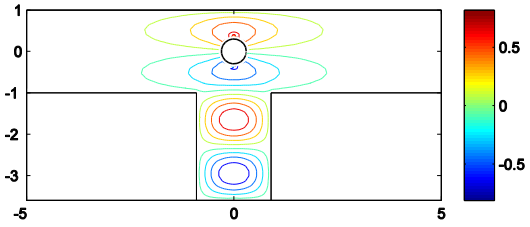

Mode No. 0.3 – 6

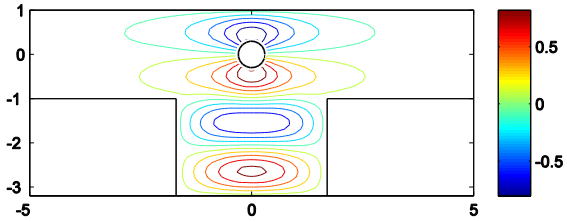

Mode No 0.3 - 11

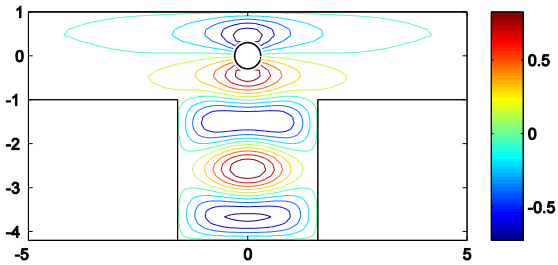

Mode No. 0.3 – 9

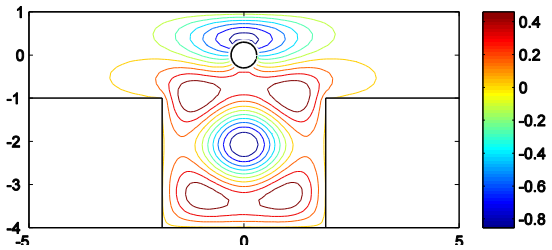

a= 0.4					
Mode No.	h	w	k	k/π	Type
0.4 - 1	0.4	3.8	2.91181	0.92686	Antisymmetric
0.4 - 2	0.6	4.2	2.72432	0.86718	Antisymmetric
0.4 - 3	0.8	4.8	2.52567	0.80395	Antisymmetric
0.4 - 4	1	3.6	3.09261	0.98441	Symmetric
0.4 - 5	1.4	3	2.64636	0.84236	Symmetric
0.4 - 6	1.4	4	2.75261	0.87618	Symmetric
0.4 - 7	1.8	4	2.83507	0.90243	Antisymmetric
0.4 - 8	2.2	3.6	2.99137	0.95218	Symmetric
0.4 - 9	2.4	4.8	2.46092	0.78333	Antisymmetric
0.4 - 10	3	3.8	2.91729	0.92860	Antisymmetric
0.4 - 11	3	3.8	2.59755	0.82683	Symmetric
0.4 - 12	3.2	1.4	2.98553	0.95033	Symmetric
0.4 - 13	3.2	5	2.46796	0.78558	Symmetric
0.4 - 14	3.2	5	2.69685	0.85843	Antisymmetric
0.4 - 15	3.4	4	2.45937	0.78284	Symmetric
0.4 - 16	3.4	3.8	2.93025	0.93273	Symmetric
0.4 - 17	3.6	2.2	2.98549	0.95031	Symmetric
0.4 - 18	3.8	2	2.95417	0.94034	Symmetric
0.4 - 19	4	4	2.67420	0.85122	Symmetric
0.4 - 20	4.4	4.2	2.53742	0.80769	Symmetric

Mode No. 04 – 3

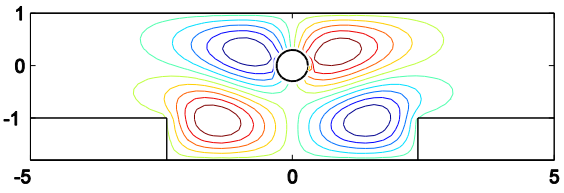

Mode No. 0.4 – 4

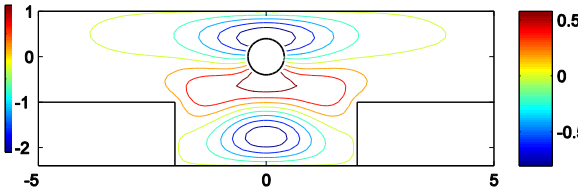

Mode No. 0.4 - 6

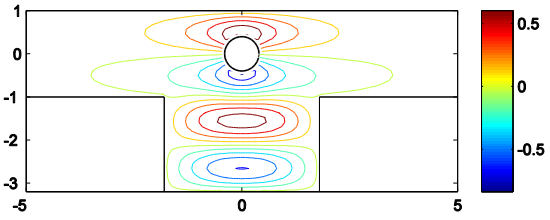

Mode No. 0.4 - 8

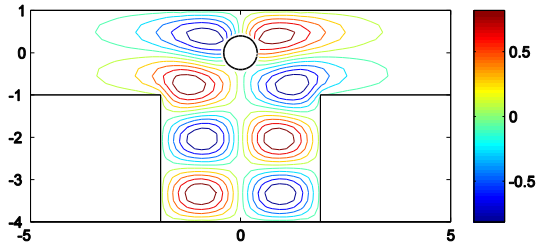

Mode 0.4 – 10

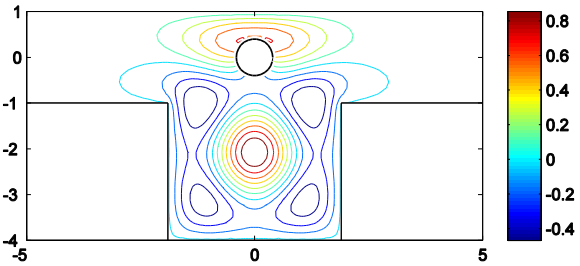

Mode 0.4 - 11

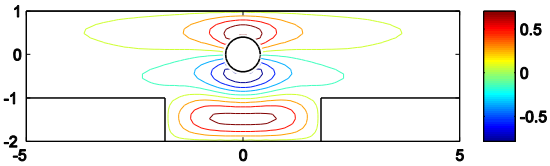

Mode No.0.4 – 16

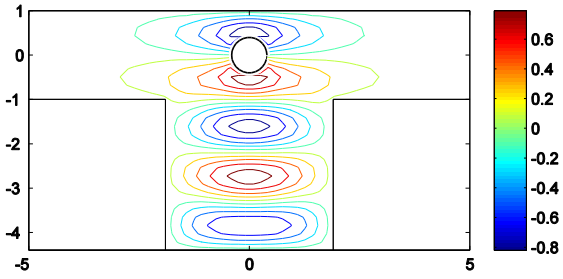

Mode No.0.4 – 20

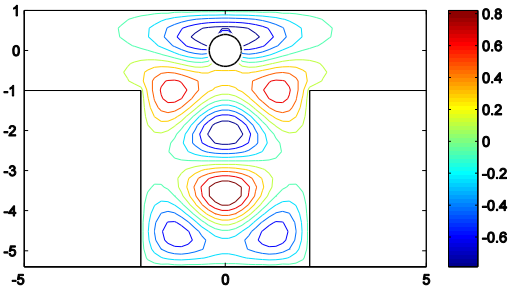

a= 0.5

Mode No.	h	w	k	k/π	Type
0.5 - 1	1.2	2	3.05683	0.97302	Symmetric
0.5 - 2	1.6	4	2.91675	0.92843	Antisymmetric
0.5 - 3	3.4	2.6	3.03562	0.96627	Symmetric
0.5 - 4	3.6	4	2.45102	0.78018	Symmetric
0.5 - 5	4	1.2	3.05626	0.97284	Symmetric
0.5 - 6	4	1.6	3.06547	0.97577	Symmetric

Mode No. 0.5 – 1

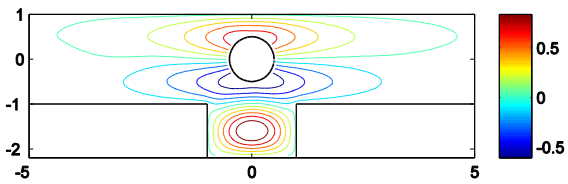

Mode No. 0.5 - 2

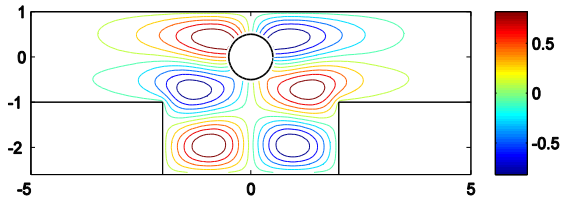

Mode No. 0.5 - 3

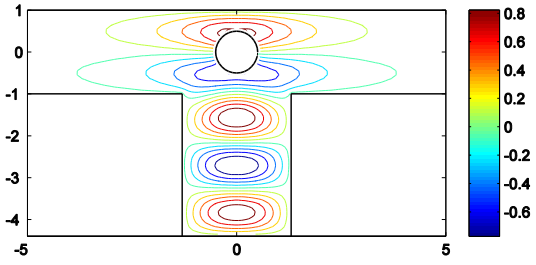

Mode No 0.5 – 4

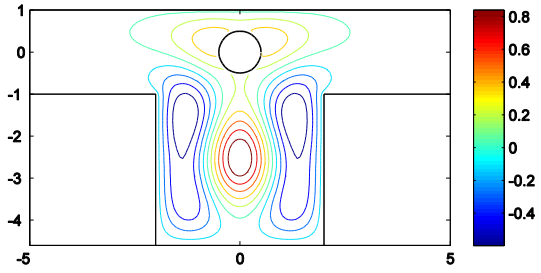

a= 0.6

Mode No.	h	w	k	k/π	Type
0.6 - 1	1.8	1.2	3.13480	0.99784	Symmetric
0.6 - 2	2.2	2.8	3.08010	0.98043	Symmetric
0.6 - 3	2.2	4	2.54860	0.81124	Symmetric
0.6 - 4	3.2	3.2	3.11298	0.99089	Symmetric
0.6 - 5	3.2	3.6	2.70943	0.86244	Symmetric
0.6 - 6	3.2	4	3.08229	0.98112	Symmetric
0.6 - 7	3.4	2.2	3.116000	0.99185	Symmetric

Mode 0.6 – 4

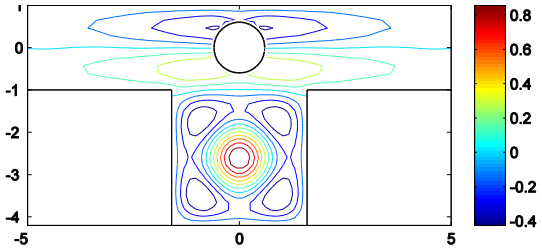

Mode No. 0.6 – 5

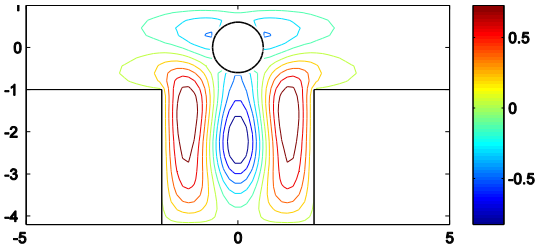

a= 0.7

Mode No.	h	w	k	k/π	Type
0.7 - 1	1.0	3	3.094245	0.98493	Symmetric
0.7 - 2	1.2	5	3.072042	0.97786	Antisymmetric
0.7 - 3	1.4	3.6	2.866064	0.91230	Symmetric
0.7 - 4	1.4	4.4	2.969265	0.94515	Antisymmetric
0.7 - 5	2.0	3	3.079549	0.98025	Symmetric
0.7 - 6	2.0	3.2	3.011674	0.95865	Symmetric
0.7 - 7	2.4	4.6	3.056370	0.97287	Antisymmetric
0.7 - 8	2.8	2.9	3.135751	0.99814	Antisymmetric
0.7 - 9	3.0	3.2	2.985512	0.95032	Symmetric
0.7 - 10	3.0	4.4	2.284029	0.72703	Symmetric

Mode No. 0.7 – 1

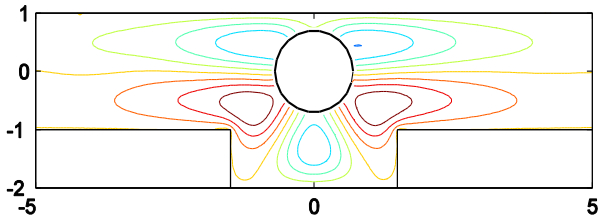

Mode 0.4 – 4

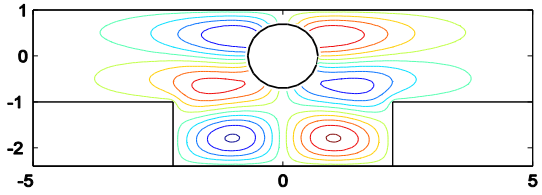

Mode No. 0.7 - 6

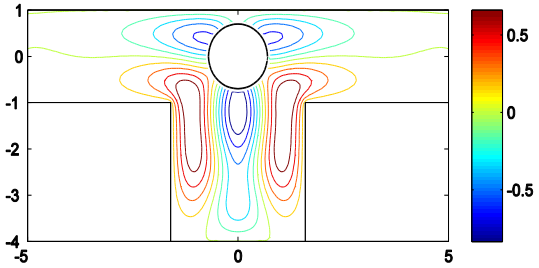

Mode No. 0.7 – 7

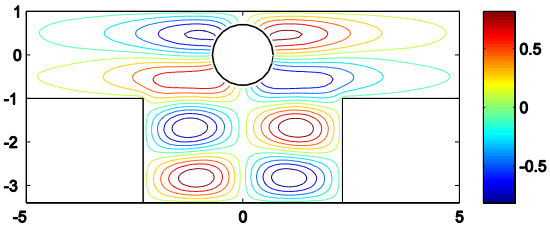

Mode 0.7 – 10

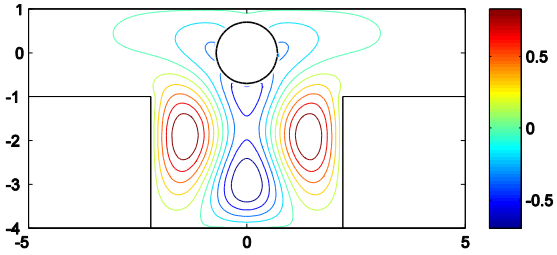

a= 0.8

Mode No	h	w	k	k/π	Type
0.8 - 1	0.8	1.2	3.006279	0.95693	Symmetric
0.8 - 2	1.2	4.4	2.60853	0.83032	Symmetric
0.8 - 3	1.4	5.8	2.90441	0.92450	Antisymmetric
0.8 - 4	1.8	5.2	2.67329	0.85093	Antisymmetric
0.8 - 5	2.8	2	3.00612	0.95688	Symmetric
0.8 - 6	2.8	5.4	3.00583	0.95679	Symmetric
0.8 - 7	3.0	4	2.48272	0.79027	Symmetric
0.8 - 8	3.0	4	2.81717	0.89673	Symmetric

Mode No. 0.8 – 1

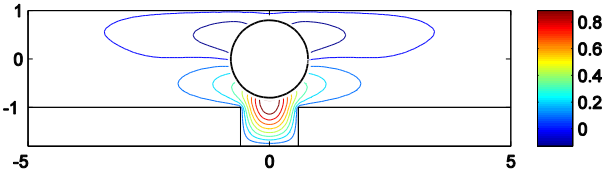

Mode No. 0.8 – 3

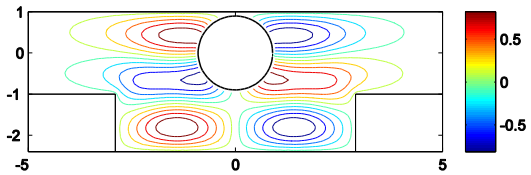

Mode No. 0.8 – 5

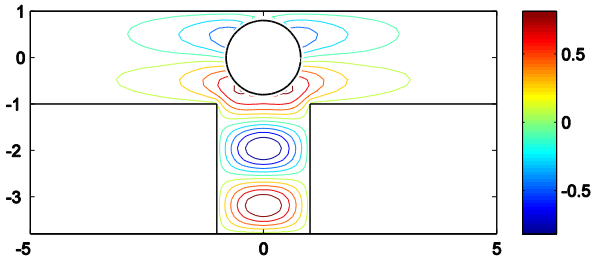

Mode 0.8 – 6

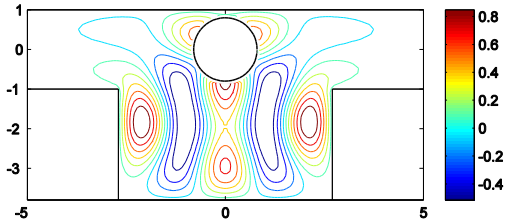

a= 0.9

Mode No.	h	w	k	k/π	Type
0.9 - 1	1.0	4.8	2.601422	0.82806	Symmetric
0.9 - 2	1.4	5.8	2.889752	0.91984	Antisymmetric
0.9 - 3	1.6	3.6	2.876110	0.91549	Symmetric
0.9 - 4	1.6	5.6	2.160214	0.68762	Symmetric
0.9 - 5	1.8	3.2	2.672035	0.85054	Symmetric
0.9 - 6	1.8	4.6	2.367837	0.75371	Symmetric
0.9 - 7	1.8	5	2.239986	0.71301	Symmetric
0.9 - 8	1.8	5.6	2.085912	0.66397	Symmetric
0.9 - 9	1.8	5.8	2.043547	0.65048	Symmetric
0.9 - 10	2.8	4	2.878430	0.91623	Symmetric
0.9 - 11	2.4	6	2.978324	0.94803	Antisymmetric

Mode No. 0.9 – 3

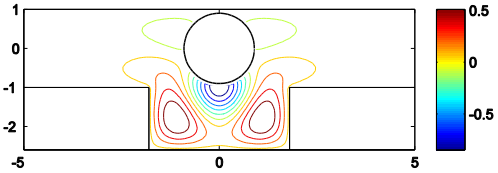

Mode No. 0.9- 5

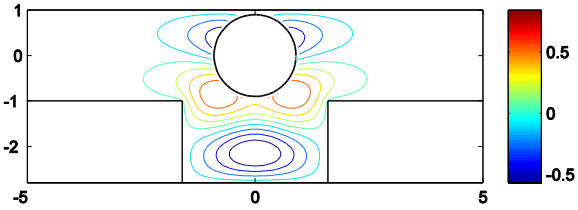

Mode No. 0.9 - 8

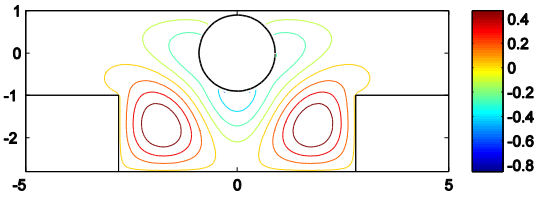

Mode No. 0.8 - 9

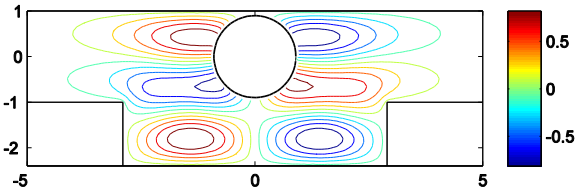

Mode No. 0.9 – 11